General report concerning some 20th century lessons and 21st century challenges in applied rock mechanics, safety and control of the environment

Rapport général concernant quelques leçons du 20ième siècle et défis du 21ième siècle en mécanique des roches appliquée et sûreté et contrôle de l'environnement

Bericht über angewandte Felsmechanik, Sicherheit und Kontrolle der Umwelt-Erfahrungen aus dem 20. Jahrhundert und Herausforderungen für das nächste Jahrhundert

NICK BARTON, Nick Barton & Associates, Oslo, Norway & Visiting Professor, USP, São Paulo, Brazil

ABSTRACT: Application of rock mechanics in civil and mining engineering is reviewed, based on perceived weaknesses and strengths, and based on the wide range of topics presented at the Paris Congress of ISRM. Arguements are put forward for making improvements in some basic areas such of stress transformation in dilatent materials, and in constitutive modelling of rock masses, both of which may be missing some basic concepts of behaviour. The wide reaching effects of dilation and anisotropic properties and boundary conditions are emphasised. Rock mass classification and empirical design is also reviewed. Such methods are the inevitable consequence both of the complexity of rock masses and of the world-wide volume of construction activities in jointed rock. Useful and simple links between classification and input data for design and verification are emphasised, using an extended Q-system and a recent development called Q_{TBM}. Continuum and discontinuum modelling are compared. It is concluded that the modelling of the components; rock, rock joints, and discontinuities is far more logical and technically relevant than present "black-box" continuum models. Excavations larger than boreholes usually mobilize joints or fabric in their response which is often anisotropic, and neglect of this represents a serious and uneccessary error. Coupled behaviour adds to the misconceptions that may be spawned by inappropriate continuum modelling

RÉSUMÉ: L'application de la mécanique des roches au génie civil et minier est passée en revue, selon les faiblesses et points forts ressentis, et la gamme étendue des sujets présentés au congrès de la SIMR à Paris. Quelques arguments sont avancés pour améliorer certains points dans des domaines de base, comme la transformation des contraintes dans les matériaux dilatants, et les lois de comportement des massifs rocheux, tous deux des domaines dans lesquels des concepts de base du comportement pourraient être manquants. Les effets innombrables de dilatation, propriétés anisotropes et conditions aux limites sont soulignés. Les systèmes de classification du massif rocheux et de la conception empirique sont aussi passés en revue. Ces méthodes sont la conséquence inévitable à la fois de la complexité des massifs rocheux, et du volume mondial de construction en milieu fissuré. Des relations simples et utiles entre méthode de classification et données d'entrée pour la conception et vérification sont soulignées, en utilisant le système Q et un récent développement appelé Q_{TBM} Des résultats de modélisation continue et discontinue sont comparés. Il est conclu que la modélisation des composants, roche, joints et discontinuités est, de beaucoup, plus logique et appropriée que les modèles existants continus type "boîte-noire". Les excavations plus larges que des trous de forage sollicitent lors de leur réponse, souvent anisotrope, les joints ou fabrique de la roche, et le fait de négliger cet aspect représente une erreur sérieuse et inutile. Les comportements couplés ajoutent aux erreurs de jugement, qu'une modélisation continue inappropriée pourrait décupler.

Zusammenfassung: Die folgende Ausführungen geben einen Überblick über Anwendung der Felsmechanik in den Bereichen Bau- und Grubeningenieurwesen, auf der Grundlage bekannter Schwächen und Stärken und im Hinblick auf die Fülle von Themen, die auf dem ISRM Kongress in Paris vorgestellt wurden. Verbesserungsvorschläge wurden in einigen Grundbereichen gemacht, wie z.B. Spannungsumlagerungen in dilatierenden Materialien und Modellierung des Spannungsdehnungsverhaltens von Fels, welche beide grundliegende Mängel in der Handhabung aufweisen können. Die weitreichenden Auswirkungen von Dilatanz, anisotropen Eigenschaften und Grenzbedingungen werden hervorgehoben. Ausserdem werden die Klassifikation von Fels und empirische Designmethoden besprochen. Solche Methoden sind eine notwendige Folge der Komplexität des Fels und des weltweiten Umfangs der Bauaktivitäten in geklüftetem Fels. Die nützliche und einfache Verbindung zwischen Klassifizierung und Eingangsdaten wird an Hand des erweiterten Q-Systems und der Neuentwicklung Q_{TBM} hervorgehoben. Kontinuierliche und diskontinuierliche Simulierungen werden verglichen. Der Autor kommt zu der Schlussfolgerung, dass die kombinierte Simulierung der Komponenten, Fels, Klüfte und Trennflächen weitaus mehr logisch und technisch relevant ist, als herkömmliche "black box" kontinuierliche Modelle. Ausschachtungen, grösser als Bohrlöcher, verursachen normalerweise eine Reaktion der Klüfte und der Matrix. Die Ausserachtlassung dieser Reaktionen stellt einen ernsthaften und unnotwendigen Fehler dar. Gekoppelte Prozesse und auf irrtümlichen Annahmen beruhende kontinuierliche Simulierungen, tragen weiterhin zum magelhaften Verständnis der oben beschriebenen Vorgänge bei.

1 INTRODUCTION

"The rock engineer of the next century will be engaged in a profession which accepts responsibility to integrate knowledge of geology, geophysics, hydrology, soil and rock mechanics, statistics, probability, and environmental sciences, with an appreciation of economics, liability, insurance, contracts, equipment design, operation, construction processes and scheduling".(After Nelson, 1996).

This long list resembles the combined expertise of key players in a rock engineering department, albeit rather a large department both in number of people and disciplines. The list

also reflects the wide range of topics that Theme 1 applied rock mechanicians may be confronted with, when travelling and attempting to give good advice on their own. Possibly it also explains why there are so many papers on so many topics in Theme 1, which my colleague Nielen Van der Merwe has bravely synthesised.

In this supplementary General Report, about twenty of the papers will be referred to in areas that are considered of key importance to the progression of our subject. These include such topics as:

- Principal stress transformation to joint and failure planes
- Input data and constitutive models
- Classification methods for estimating rock mass properties
- TBM tunnelling in jointed and faulted rock
- Grouting of jointed rock
- Discontinuum modelling and anisotropy

Some 25 years ago, in South Africa, the writer as a panelist was asked what is the most important property in rock engineering? His answer was joint *dilation* during shearing. As will be seen in a moment, there may be more justification in this choice than was apparent to anyone at the time.

Today, if given a second choice, the word *anisotropy* would be added to the list of most important properties. The anisotropy of fabric, joint structure and stress, and the resulting anisotropic rock mass properties (including permeability) are fundamental to our subject, but are tending to be forgotten in all too popular continuum modelling, where only anisotropic stress may be applied due to time and budgetary constraints, laziness, or incorrect assumptions.

2 PRINCIPAL STRESS TRANSFORMATION TO JOINT AND FAILURE PLANES

A fundamental aspect of applied rock mechanics and a safety issue of considerable importance is stress transformation in slopes, dam abutments and around tunnels and caverns.

Transformation of principle stresses σ_1 and σ_2 into shear (τ) and normal stress (σ_n) components along an imaginary plane that does not shear, or dilate (or even exist) seems to be universally based on Mohr's theory, (1882).

The components τ and σ_n are usually calculated as follows:

$$\sigma_n = \tfrac{1}{2}(\sigma_1 + \sigma_2) - \tfrac{1}{2}(\sigma_1 - \sigma_2)\cos 2\beta \quad (1)$$

$$\tau = \tfrac{1}{2}(\sigma_1 - \sigma_2)\sin 2\beta \quad (2)$$

where $\beta°$ = angle between the σ_1 direction and the imaginary plane.

The problem faced in rock and soil engineering is that joints or failure surfaces do exist (or will exist with sufficient shear strain), and in many materials they also dilate. Most rock joints dilate when sheared unless very plane and smooth. Compacted silt, sand, gravel, rock fill and over-consolidated clay also dilate, unless each are sheared under unusually high levels of stress.

When dilation occurs shear stress and shear strain are no longer co-axial. Both in soil and rock mechanics, our use of Mohr theory is then incorrect.

Protests will arise that both the soil and rock mechanics communities are well aware of the need for energy corrections, that constant (normal) stress and constant (normal) stiffness boundary conditions beneath slopes and around tunnels are correctly differentiated and accounted for. We also correct the mechanical joint apertures by the dilation that has occurred, and convert the result to an increased hydraulic aperture (e.g. Barton et al. 1985). The problem is that dilation is not only a question of aperture increase and normal stress increase.

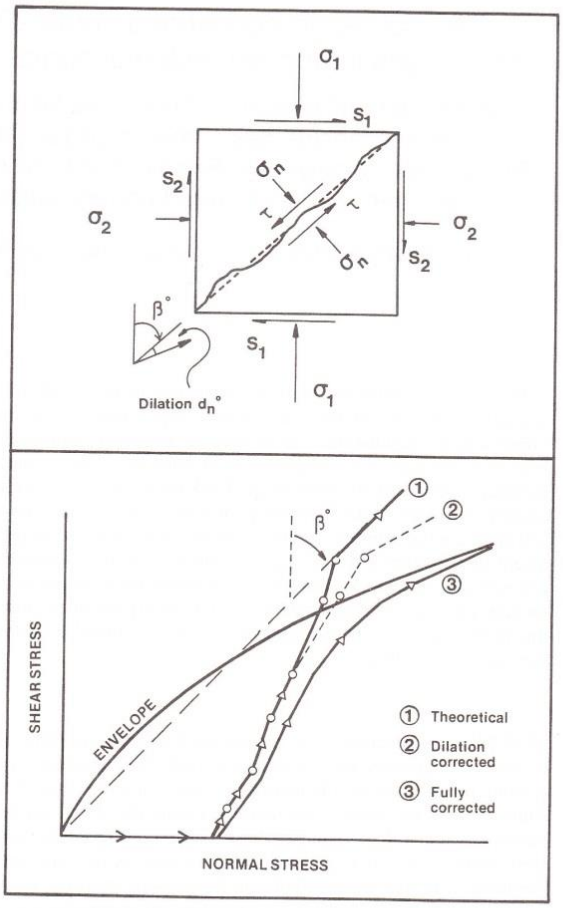

Figure 1. Biaxial shear testing of diagonally jointed samples runs into problems of incorrect application of Mohr stress transformation, due to non-coaxial stress and strain. Bakhtar and Barton, 1984, Barton 1986.

In 1983, a close friend and former colleague, Dr.Khosrow Bakhtar and the writer attempted to shear eight, $1m^3$, diagonally jointed blocks of sandstone, tuff, concrete and hydrostone in a large flatjack-loaded biaxial frame, (Bakhtar and Barton, 1984). Tilt tests under self-weight loading had previously given full scale JRC_n (joint roughness coefficients) varying from 4.2 to 10.7 for these 1.3 to 1.4 m long jointed samples. The test set- up is shown schematically in Figure 1 (top). The assured τ-σ_n stress path (line 1) in Figure 1 (bottom) was shown to far exceed the calculated failure envelope, when stress transformation was based on equations 1 and 2.

Due to the (usually) robust nature of our jointed samples, it is often possible in rock mechanics to perform non-destructive index tests on joint samples prior to shearing the same samples at elevated stresses in biaxial test frames, as illustrated in Figure 1, or in direct shear boxes.

Our ability to predict the shear strength of joints is illustrated in Figure 2 and is based on tilt tests, and Schmidt hammer tests, with verification by direct shear testing. Results of predicted strength and measured (shear box) strength for more than 100 joint samples are given in Figure 3. (Barton and Choubey, 1977).

Mean predicted ϕ_{peak} = 45.6° (from tilt testing)
Mean measured ϕ_{peak} = 45.1° (from shear box testing)

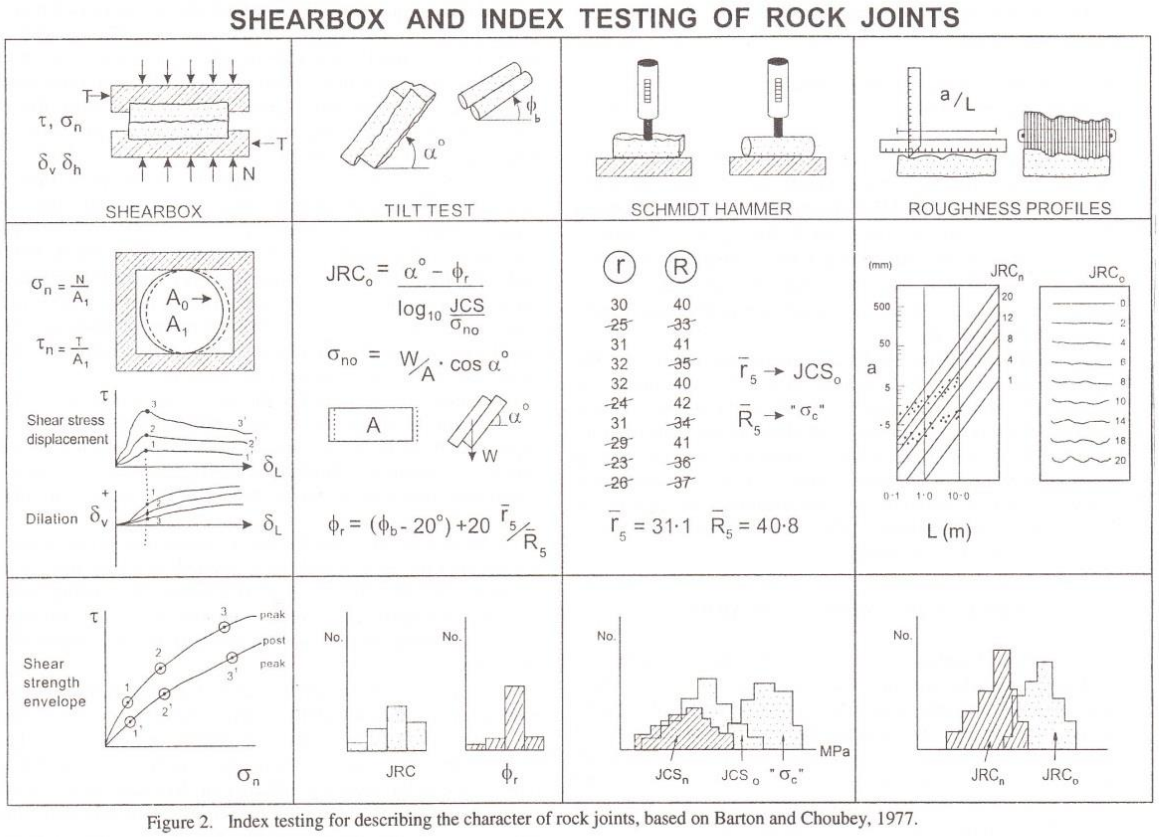

Figure 2. Index testing for describing the character of rock joints, based on Barton and Choubey, 1977.

In contrast to Figure 3, a remarkably poor set of measured and predicted data shown in Figure 4 from Gale et al. (1993) prompted Gale to suggest a modification to the "JRC-JCS or Barton – Bandis model. In fact the consistent error (all measured strengths are higher than predicted) is due to the same problem of stress transformation as in Figure 1, because a novel hydraulic biaxial loading system was also used by Gale, and required stress transformation to the 45° inclined joints, unlike in a conventional shear box where the joints are parallel to σ_1 or σ_2.

A possible solution to the incorrect Mohr stress transformation is the inclusion of the mobilized dilation angle ($d_{n\,mob}$) which can be calculated following Barton, 1982. This angle is stress, displacement and size dependent, and has a flat-S shape when plotted from data on normal and shear displacements.

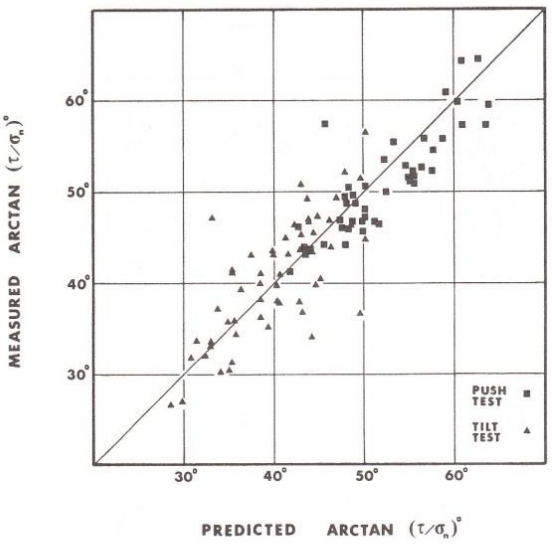

Figure 3. Prediction of peak shear strength based on JRC, JCS and ϕ_b measurement, and comparison with direct shear test data. After Barton and Choubey, (1997).

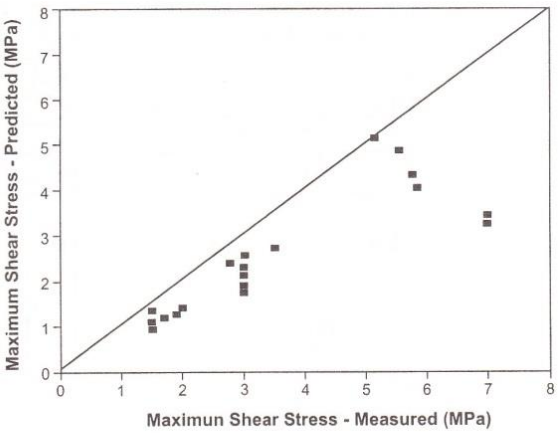

Figure 4. Comparison of the peak shear stress computed using JRC, JCS, and ϕ_r index test data, with the maximum shear stress determined experimentally, using a biaxially loaded, novel shear box. Gale et al., 1993.

The dilation corrected stress transformation, as utilized by Bakhtar and Barton (1984), is as follows.

$$\sigma_n = ½ (\sigma_1+\sigma_2) - ½ (\sigma_1-\sigma_2) \cos 2 (\beta+d_{n\ mob}) \quad (3)$$
$$\tau = ½ (\sigma_1-\sigma_2) \sin 2 (\beta+d_{n\ mob}) \quad (4)$$

The inclusion of $d_{n\ mob}$ in the non-coaxial stress transformation suggested by equation 3 and 4 means that σ_n will always be higher than calculated by Mohr theory, while τ will be higher if $(\beta+d_{n\ mob}) < 45°$, and τ will be lower if $(\beta+d_{n\ mob}) > 45°$. Since $\beta = 45°$ in a typical biaxial loading frame (flatjack or hydraulic cylinder loading), the ratio τ/σ_n that one assumes is being applied to the diagonal (β=45°) joint is actually significantly lower in the real world.

This 100 years error nearly caused serious injury in 1983 when one of our large 1m^2 flat jack burst at 28 MPa, due to the refusal of a non-planar joint to follow Mohr theory. All the samples tested by Gale (Figure 4) are showing the same need for some form of mobilized dilation correction. A wide-ranging need for corrections is apparent in both rock and soil mechanics, wherever dilatant materials and deformations are significant. (e.g. Gutierrez and Ishihara, 1999). There is much work to be done as we enter the next century.

3 INPUT DATA AND CONSTITUTIVE MODELS

Several Theme 1 authors have reported the results of numerical models of tunnels, caverns and rock slopes. We will hear individual presentations of several of these during the discussion period. Interesting two-dimensional and three-dimensional approaches using both continuum and discontinuum methods are described, with occasional use of both deterministic and stochastic joint representation (e.g. Barla et al., 1999, Hakala et al., 1999, Dasgupta et al., 1999 and Jang et al., 1999, to name just four).

Without wishing to single out any individual paper, a general question and important issue must nevertheless be raised as we leave at least forty years of rock engineering developments from the 20th century, and ponder the best ways to proceed in the next century.

The critical questions concern both the relevance of strength and deformation parameters, and the relevance of the models in which they are used. Should we believe in one value of c (often given to two decimal places) and one value of ϕ° for those parts of a rock mass that have been given specific Hoek-Brown parameters and truncated Q or RMR values ?(i.e. Q′or RMR′, or GSI) (Hoek and Brown, 1997)

Is it defensible to ignore the frequently anisotropic pattern of jointing and stress distribution and their combined effect on input parameters? Is it defensible to base rock mass strength estimates on intact rock, curve fitted parameters, c and ϕ, and m and s that have little physical meaning? Is it defensible to ignore the warnings of the originators of the Hoek - Brown criterion for rock masses, that it should only be used when the block sizes are small compared to the size of excavation, or when the properties of the rock mass are the same in all directions?

Judging by the frequency of the use of continuum models, the writer begins to suspect that he has a wrong impression about the typical nature of most rock masses. In fact most rock masses and boundary conditions should disqualify the use of isotropic continuum modelling and associated equal-in-all-directions input data.

A Mohr Coulomb based c and ϕ formulation, or an m and s formulation for the isotropic shear strength of a rock mass is an avoidance of the real behaviour, if cohesionless jointing which also does not satisfy the limited conditions of isotropy discussed above, is indeed present as it so often is in rock engineering problems.

Even in a two-dimensional case, and using just three simple joint structures, the potentially widely different load-deformation behaviour shown in Figure 5 must be apparent. The displacement Δ increases dramatically from type A to type B to type C, due to the reducing influence of the intact rock, and the increasing influence of the joint properties as one proceeds from left to right in this figure. For this reason the ratios of K_n/K_s (peak) and K_n/K_s (residual) tend to be large and very large respectively, and are therefore highly anisotropic, as any observer of a wedge failure must surely acknowledge.

If one accepts that rock mass behaviour is frequently dominated by joint behaviour as opposed to modified intact rock

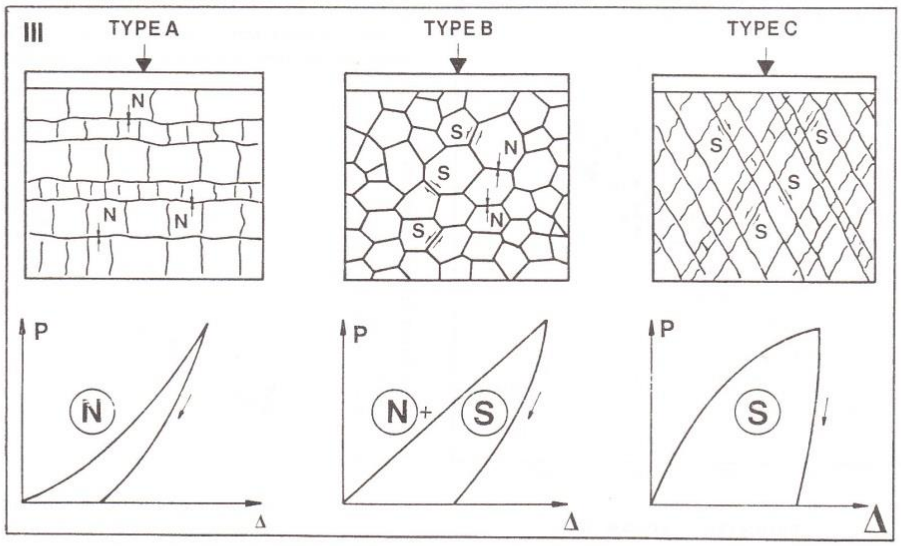

Figure 5. Normal closure (N) and shear displacement (S) components of behaviour, and their potential influence on rock mass load-deformation behaviour. (Bandis 1980 and Barton 1986).

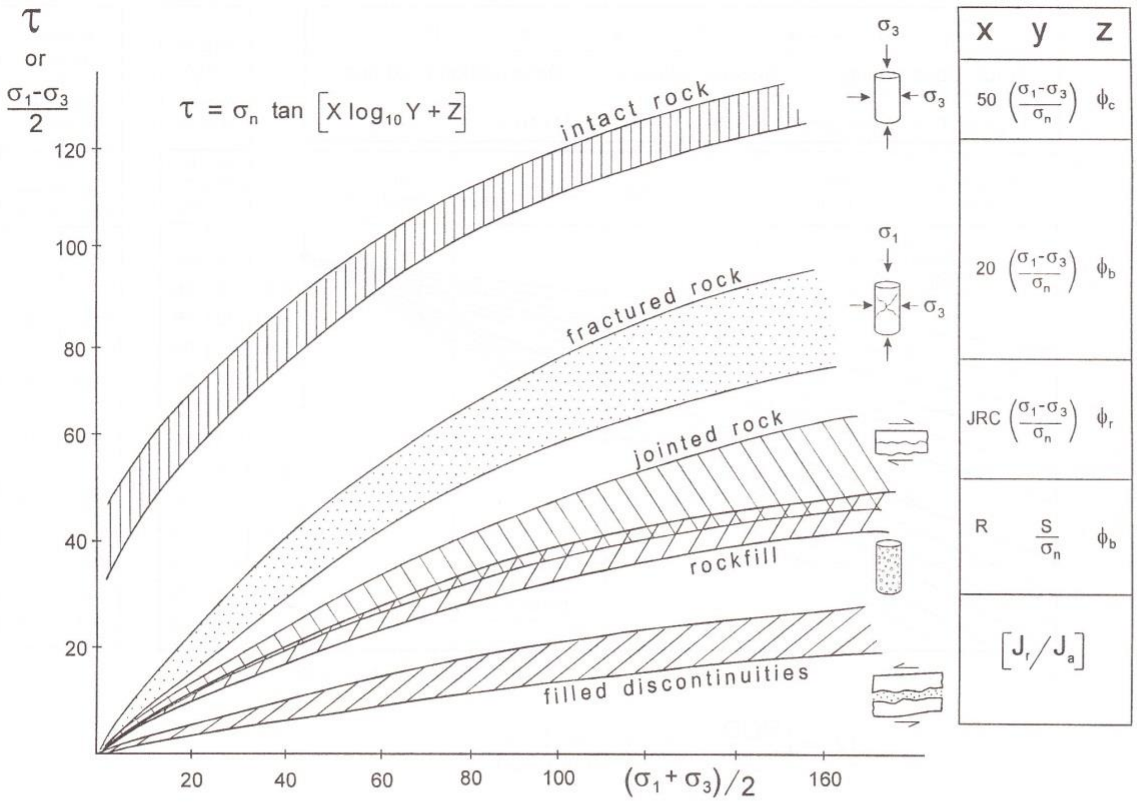

Figure 6. Five components of rock mass shear strength (intact, fractured, jointed, crushed, filled discontinuities). From Barton 1976, Barton and Choubey 1977, Barton and Kjærnsli 1981 and Barton et al., 1974.

curve fitting, (c and ø, and m and s) then an alternative and probably more logical approach would surely be the use of joint strength and joint deformation formulations from the outset.

Easily understood empirical equations for fitting and partially explaining the shear behaviour of fractured and jointed rock have been assembled in Figure 6. The empirically based $\log_{10}$ term is needed due (amongst other reasons) to the great mismatch between the real contact-area ($A_1 \approx \sigma_n$/JCS x 100%) and the assumed contact area (A_o =100%).

The derivation of necessary input data concerning JRC, JCS, ϕ_r and ϕ_b is illustrated by the index tests shown in Figure 2. Equivalent index test methods for estimating R and S for gravel and full scale rockfill (i.e. crushed rock) were described by Barton and Kjærnsli 1981. They have been performed with sample sizes up to 5 m in length at a dam site in Italy. The even more simple formulation for filled joints is based on the Q-system parameters J_r and J_a (Barton, 1995).

An alternative formulation for intact rock in terms of σ_1 and σ_3 is the linear form:

$$\frac{\sigma_1 - \sigma_3}{\sigma_c} = M(\sigma_3 / \sigma_1) + 1 \cdot 0 \qquad (5)$$

which shows linearity at least up to the brittle-ductile transition (Barton, 1976). As examples, the gradient M is 3 for Solenhofen limestone, 7 for Oak Hall limestone, 9 for Nahant grabbro and 30 for Westerly granite.

It should be noted that the X terms in Figure 6 (R, JRC, 20) specifically represent roughness, (the "i" value in a ϕ + i formulation) while the Y terms (S, JCS, σ_1 - σ_3) specifically represent the effective compressive strengths, which are compared with the mean, assumed normal stress in each case. The basic and residual friction terms ϕ_b and ϕ_r also have specific physical meaning. With the exception of the intact rock formulation, which is purely curve-fitting (Barton, 1976) the other formulae listed in Figure 6 simply need individual physical index tests to obtain their magnitudes. Curve-fitting is not involved, isotropy is not expected, and discontinuum modelling is essential. Perhaps we should try to apply and refine such approaches in the next century.

4 CLASSIFICATION METHODS FOR ESTIMATING ROCK MASS PROPERTIES

Two widely used classification methods developed in the early seventies (Bieniawski, 1973 and Barton et al. 1974) have also been subject to misuse, just as the Mohr Coulomb and Hoek and Brown criteria have for rock masses. However, the classification methods probably can be said to have served a useful purpose when communicating and interpreting different conditions, even though subjective differences in interpretation (as discussed by Escoffier et al. 1999 in this congress) can be demonstrated, to varying degrees. Much discussion has ensued since RMR and Q were developed, and even some lawyers are beginning to know that RMR = 30 is not the same as Q ≈ 30

Right from the start, and at least up to recent times (Bieniawski, 1989 and Barton and Grimstad, 1994) these methods have retained a "linear" scale and a "logarithmic" scale respectively. Stress has always been absent from RMR, but present indirectly, from the ratio σ_c/σ_1 needed for estimating

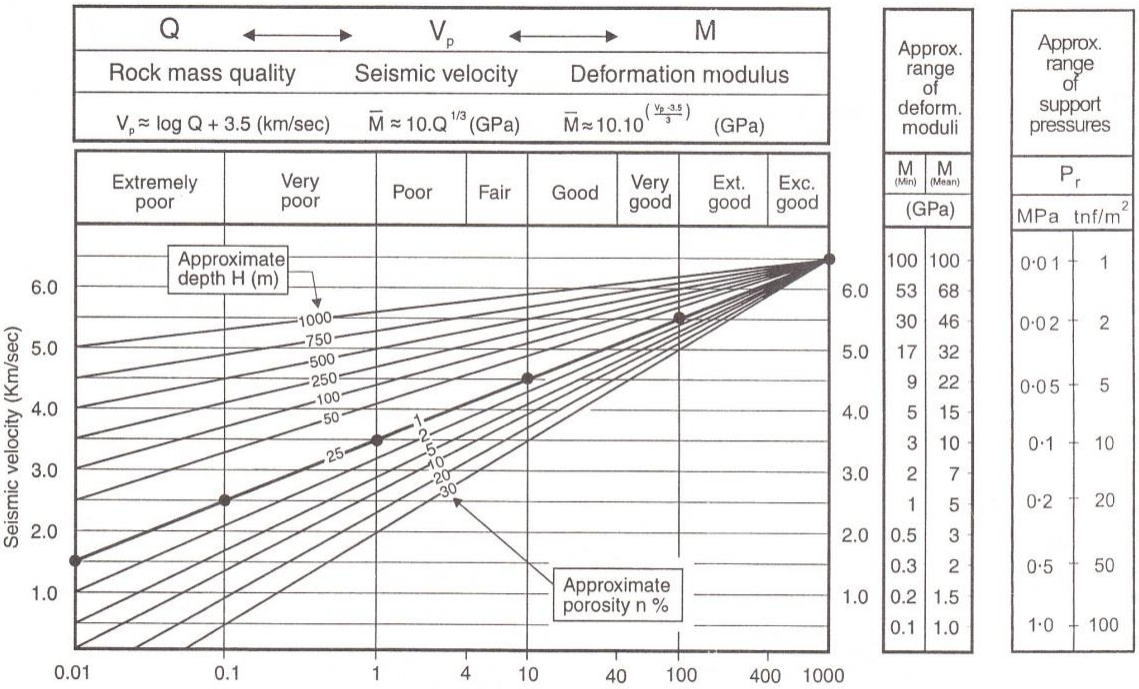

$$Q_c = \left(\frac{RQD}{J_n} \times \frac{J_r}{J_a} \times \frac{J_w}{SRF}\right)\frac{\sigma_c}{100}$$

Figure 7. Chart for estimating inter-relationship between Q, V_p, M, P_r, σ_c, n and H , after Barton, 1999a).

SRF in the Q-value. Concerning orientation or anisotropy, average joint properties seem to be used for RMR, but corrections for favourable or unfavourable orientations are made.

In the case of the Q-system, the joint roughness and alteration (filling) parameters J_r and J_a are specifically meant for the joints or discontinuities that are least favourable to tunnel or cavern stability. Orientation and a form of "limit equilibrium" based parameter rating is involved in the Q-value, since from the start the values of each parameter were developed by trial and error from more than 200 case records, trying to match the Q-parameter ratings with the rock reinforcement needs.

The "limit-equilibrium" aspect of the Q-value, and its logarithmic (six order of magnitude) scale are probably the reasons why very simple relations to widely varying rock mass parameters are found, of which the following approximations have been reported since 1974:

$P_r \approx 0.1Q^{-1/3}$ (MPa) (6)

$M \approx 10Q_c^{1/3}$ (GPa) (7)

$V_p \approx 3{\cdot}5 + \log Q_c$ (km/sec) (8)

$\Delta \approx \frac{SPAN(m)}{Q}$ (mm) (9)

$L \approx 1/Q_c$ (l/min/m/10atm.ΔP) (10)

where P_r = radial support pressure (in tunnel or cavern)
M = rock mass deformation modulus
$Q_c = Q \times \sigma_c/100$
σ_c = uniaxial compression strength
V_p = P-wave velocity from shallow refraction seismic (e.g. 25 m depth)
Δ = tunnel or cavern deformation
L = Lugeon (high pressure water injection) test value

Some comments will be made on each of the above relationships, in order to demonstrate the practical value of the Q or Q_c number in applied rock mechanics. Where appropriate, references will also be made to papers presented in this session of the ISRM Congress.

4.1 V_p–Q and depth effects

The inter relationship between seismic velocity and Q-value (equation 8) is shown by the central trend line in Figure 7. (Nominal 25 m depth and 1% porosity). Velocity is increased by depth increases (in a strongly non-linear manner) and is reduced by porosity increases (in a more linear manner). The use of Q_c when the uniaxial strength differs from the nominal 100 MPa for hard rock completes the V_p-Q_c-depth-porosity inter relationship shown in Figure 7. Details of its development are given by Barton 2000a.

When interpreting seismic velocity data such as the interesting sets of data presented by Chikahisa et al. (1999) for the Japanese art exhibition done of 40 m span, the registered velocity of say 4·8 km/sec for the C_H class welded tuff can be converted to a Q_c-value and then to a Q-value, by reading off the depth, porosity and uniaxial compression strength. In the case of ultrasonic measurements performed in bolt or anchor holes surrounding an excavation, as reported by the same authors, the appropriate stress level would be used to interpret the equivalent depth term. Disturbed zone velocities, which may vary strongly with depth, can then be converted to Q-values which would

show less variation with depth, as is usually appropriate to the moderate levels of blast damage.

An interesting paper by Savich et al. (1999) to this session, shows tomographic seismic velocity in the foundation of the Ingouri dam following many years of monitoring. Systematic non-linear increases in velocity are shown (e.g. 4.0 to 4.8 km/sec) as reservoir level is increased by nearly 100 meters. When reservoir level drops, hysteresis is seen.

4.2 V_p-Q-support pressure

The radial support pressure interpreted from bolt and anchor capacities and given by equation 6, is based on Barton et al. 1974, with the assumption that the ratio 2/Jr appearing in the original equation can often be approximated to unity (i.e. when Jr = 2 for smoothy undulating joints). In view of the approximation given in equation 6, the simple support pressure estimate given in the right hand side of the Figure 7 should correlate with the seismic velocity V_p. We may then conjecture that the normalized version of Q_c (=Q x σ_c/100) may be a defensible improvement to equation 6 for the case of weak or hard rock, i.e.:

$$P_r \approx 10\, Q_c^{-1/3} \quad (\text{tnf/m}^2) \qquad (11)$$

It is interesting to note that this has an inverse relationship to the rock mass deformation modulus (equation 7), which seems inherently reasonable, i.e.

$$P_r \,\alpha\, 1/M \qquad (12)$$

In conventional units, as shown to the right hand side of Figure 7:

$$P_r \approx 100/M \qquad (13)$$

(where P_r is in units of tnf/m^2, M is in GPa).

Modulus reduction in the excavation disturbed zone will be one reason for P_r to increase. However, until squeezing or stress slabbing occurs, a reduced support pressure will initially be registered as depth increases, due to the higher modulus.

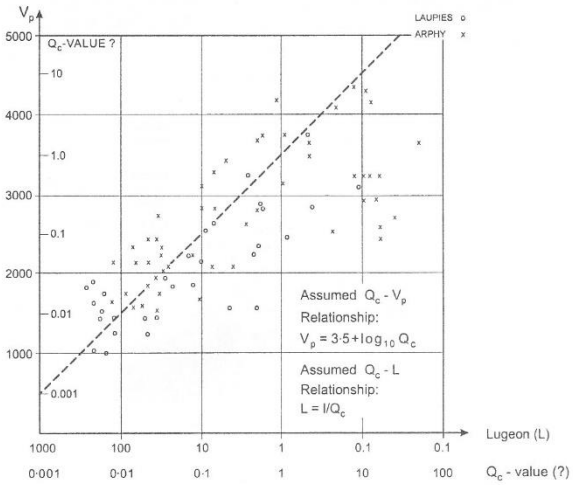

Figure 8. V_p-Lugeon data for two dam sites in France (French Group, ICOLD, 1964). The Q_c scales and trend line (equation 10) have been added by Barton, 1999a.

4.3 V_p-Q-Lugeon

Equation 10 relating the Q_c-value with the Lugeon value, is a recent lower bound approximation, that was initially suggested by the V_p-Lugeon data shown in Figure 8 for two dam sites in France. Perhaps suprisingly there is some theoretical justification for this simple inter-relationship, when the Lugeon test is interpreted as a deformation test. Ten atmospheres (1MPa) excess water pressure as applied in the Lugeon test, represents a significant reduction in effective stress in the single joint, or joints set, or joint sets that are directly affected.

Sympathetic closure of joints not similarly penetrated by the raised water pressure, gives the space required for hydraulic jacking of some of the joints. When a particular joint aperture becomes large, the aperture E, when cubed, may dominate the total measured flow. The proportionalities shown in Figure 9 (inset) when utilized in a radial flow approximation can be shown to approximate equation 10 ($L \approx 1/Q_c$).Use is made of a classic Boussinesque approximation for circular loading of each side of the dominant (most permeable and easily jacked) joint to derive this simple relationship from radial flow assumptions. (Barton, 1999a).

The chart shown in Figure 9 is a direct derivation of Figure 7, with Q_c and Lugeon scales (each obviously approximate) added along the axes. One may observe that the usual approximation ($L \approx 10^{-7}$ m/sec) suggests a six order of magnitude scale from 10^{-4} m/sec to 10^{-10} m/sec from worst rock mass quality to best rock mass quality. Note the avoidance of the use of the term "permeability" in view of the fact that a Lugeon test is a deforming test in near–surface situations, where total stresses are not much higher than the injection pressure. Aspects of grouting and joint aperture assumptions discussed by Eriksson et al. (1999) in this session of the Congress, will be discussed later in this General Report.

4.4 Type curves for rock masses

Accepting that approximations are acceptable, and usually more relevant to our subject than two decimal place accuracy, the chart in Figure 9 can be used to present possible "type curves" for rock masses of different character, excavated at different depths. The weathering effects will be represented by an increase in porosity at shallow depth.

Widely different rock mass qualities (Q_c), deformabilities (M), velocities (V_p) and approximate Lugeon values are predicted for the five cases illustrated in Figure 9.

- hard massive rock (unweathered)
- hard jointed rock (slightly weathered)
- weak porous rock (deeply weathered)
- minor fault (deep alteration)
- major fault (deep alteration and weathering)

Exceptions to these general trends will be useful points for discussion and may require explanation, and can help to bring improved understanding of rock mass variability, which is truely a "parameter" of our subject.

4.5 Tunnel deformation and Q

Comparison of measured displacements with numerically predicted ones is a common way of verifying the applicability of computer codes, or demonstrating the needs for adjustments of input data. Sometimes adjustments to input data are seen to be most necessary in the excavation disturbed zone. However a simple reduction of modulus surrounding an excavation may introduce its own set of problems in a continuum model, if stresses are anisotropic.

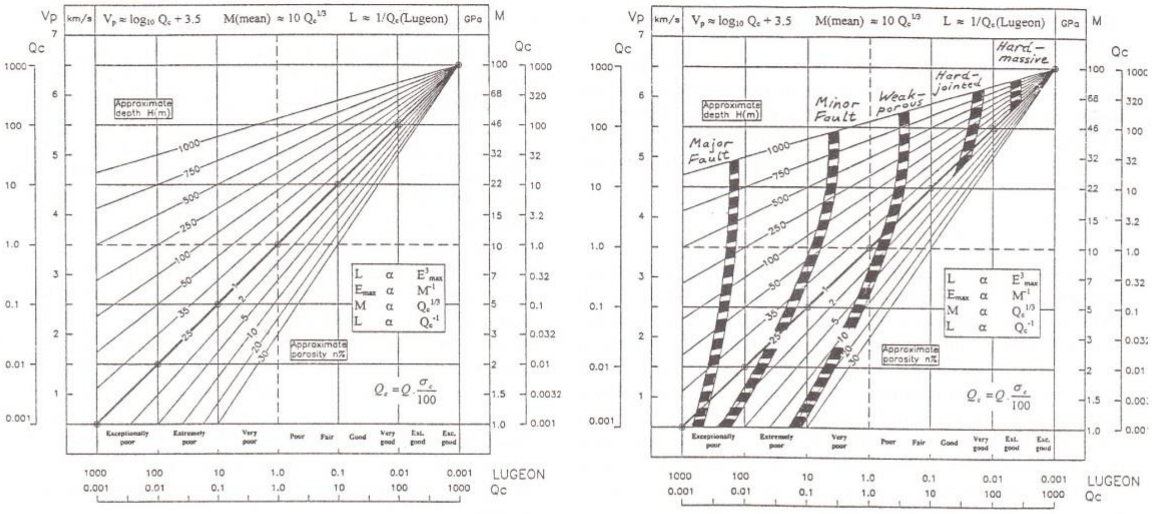

Figure 9. Integration of some static, dynamic and hydraulic properties (in approximate terms) and rock mass qualities, to show the potential of *type curves* for describing possible ranges of behaviour.

Three-dimensional discontinuum (3 DEC) models reported by Hakala et al. 1999 and Dasgupta et al. (1999) in this session of the ISRM Congress show some remarkable similarities to measured data when input data is updated during excavation, and less good fit when the input data (and geometry, are based on pilot tunnel mapping). Each of these results is to be expected.

Since one cannot perform enough numerical predictions of displacement for verifying the adequacy of rock support in relation to the thousands of kilometres of tunnels driven every year, empirical approaches are also necessary, and these perhaps deserve less criticism than occurs from some quarters. They can also be used as a form of preliminary verification of a numerical model.

The two sets of tunnel and cavern deformation data shown in Figure 10, show a central trend of:

$$\Delta\,(\text{mm}) = \frac{SPAN(m)}{Q} \tag{14}$$

The data includes numerous hard and soft rocks from Scandinavia, Europe, and especially Taiwan (Chen and Guo, 1997) and excavation spans range from about 4 to 60 meters. While some of the scatter is undoubtedly due to insufficient or too conservative support, a certain amount can be ascribed to "geotechnical" scatter, or to the need for more direct input data than appears in the Q-value.

The ratio of stress to strength, used in many parts of the world and in both soil and rock mechanics, has been added in what follows. Stress (σ_v or σ_h) and strength (σ_c) are given in consistent units (i.e. MPa) and deformation (Δ_v or Δ_h) are given in millimeters together with dimensions SPAN or HEIGHT. The following is proposed:

$$\Delta_v \approx \frac{SPAN}{100.Q}\sqrt{\frac{\sigma_v}{\sigma_c}} \tag{15}$$

$$\Delta_h \approx \frac{HEIGHT}{100.Q}\sqrt{\frac{\sigma_h}{\sigma_c}} \tag{16}$$

The stress anisotropy Ko ($= \sigma_h/\sigma_v$) can therefor be expressed simply as:

$$\text{Ko} \approx \left(\frac{\Delta_h}{\Delta_v}\right)^2 \left(\frac{SPAN}{HEIGHT}\right)^2 \tag{17}$$

For example the Gjøvik cavern with span of about 60 m (60,000 mm) showed a total "radial" arch deformation of about 6 to 8 mm, and had a mean Q-value of about 10. The average depth was 40 m (say σ_v = 1 MPa) and the average uniaxial strength σ_c

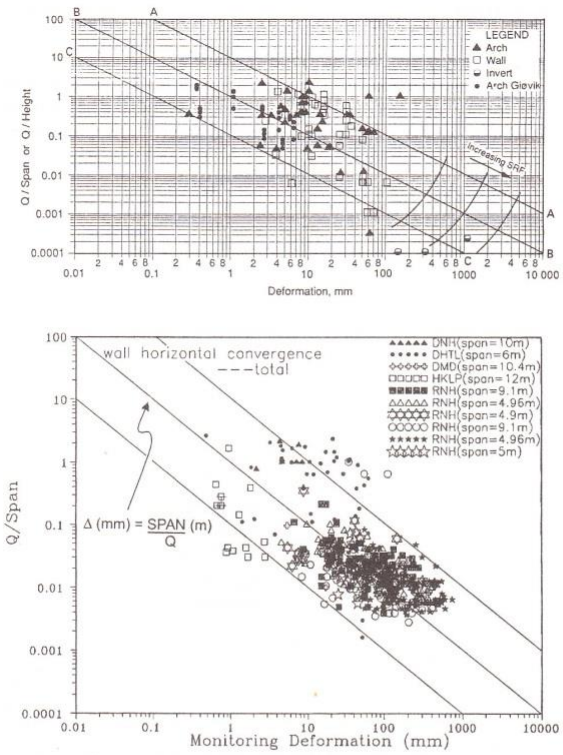

Figure 10. Q/span versus deformation data for tunnels and caverns from Barton et al., 1994 and Chen and Guo, 1997.

≈ 75 MPa (tectonised gneiss). Substituting in equation 15 one obtains:

$$7\ \text{mm} \approx \frac{60{,}000}{100 \cdot 10}\sqrt{\frac{1}{75}}$$

The right hand side of this approximation is calculated to be 6.9 mm. Normally the agreement would not of course be as close as this. The influence of horizontal stress on Δ_v is also unknown in this case.

We can also test these equations against the recently constructed Nathpa Jhakri power house in India. The following measured data has been used in numerical UDEC-BB modelling of this cavern, reported by Chryssanthkis et al. (1996) and Bhasin et al. 1996.

Span ≈ 20 m $\sigma_v \approx 6$ MPa $\sigma_c \approx 35$ MPa
Heigh ≈ 50 m $\sigma_h \approx 4$MPa (perpendicular to wall) Q ≈ 3

Measured deformations (where MPBX are installed) are approximately 25 mm in the arch and up to approximately 50-55 mm in the walls, though there is significant variability here. Equations 15 and 16 give the following excellent estimates:

$$\Delta_v \approx \frac{20{,}000}{10 \cdot 3}\sqrt{\frac{6}{35}} \approx 28mm$$

$$\Delta_h \approx \frac{50{,}000}{10 \cdot 3}\sqrt{\frac{4}{35}} \approx 56mm$$

With these Natpa Jhakri power house predictions we therefore have:

$$K_o \approx \left(\frac{56}{28}\right)^2\left(\frac{20}{50}\right)^2 \approx 0.64$$

Measured values of the principal stresses were $\sigma_h \approx 4$ MPa, $\sigma_v \approx$ 6 MPa, i.e. almost the correct result is shown.

4.6 Truncating of rock quality classification methods

The methods illustrated above, represented by the main parameters Vp, Q, M, and Δ, can represent powerful tools for applying rock mechanics principles in design, for checking the results of numerical modelling, and for interpreting and perhaps reacting to monitoring data. However, before leaving the subject of rock mass classification, the late 20th century trend of truncating parameters such as Q′ (minus J_w and SRF) and RMR′ (minus water) must be commented upon. This trend of course follows chronologically the reversed tendency to add parameters to RQD that occurred in the early 1970's!

Even the use of only RQD/J_n to represent relative block size, for correlation with potential slope failure modes is demonstrated in an interesting analysis by Glastonbury et al. 1999 in this session. There was some indication of failure modes changing from toppling to sliding to mass failure (rotational) as RQD/J_n (as a proportion of the size of the failure) decreased. The authors also found that the maximum strain before collapse was more or less proportional to the "linear" RMR quality scale (in RMR range of 25 to 65). Failure volumes investigated varied from 3000 m^3 to a huge 18,000,000 m^3.

The Canadian mining industry has for many years made use of the truncated $Q' = RQD/J_n \times J_r/J_a$ ("block size" times "inter-block shear strength") in an empirical approach to stope design (e.g. Potvin et al. 1989) commonly known as the Matthews approach. Ignoring J_w and SRF is perhaps acceptable if water, shear zones and faults are seldom encountered. However, as pointed out by Goel and Wezenberg (1999) in this session, such methods will not be applicable when there are influences from shears, faults and clay layers, as experienced in the Ashanti gold fields. The term SRF, though complex for the weak-hearted, is an essential modifier of quality, and its omission prevents the use of the empirical design tools summarized in the foregoing sections of this report.

For statistical calculations, such as Kriging, Syrajänen and Lovén (1999) found that the normal distributions of rock class (such as RMR or the Hoek et al. 1995 GSI value) were easier to interpret than log normal distributions such as Q.

4.7 Inter-relation between Q and RMR for tunnel support estimation

The following standard form of conversion between GSI and Q′ which was previously used between the complete RMR value and the complete Q value (Bieniawski, 1989) has a tendency to predict vanishing and even negative values at low values of RMR or RMR′.

$$GSI = 9 \ln Q' + 44 \qquad (18)$$

For this reason, the $\log_{10}$ form illustrated in Figure 11 is preferred (Barton, 1995).

$$RMR \approx 50 + 15 \log_{10} Q \qquad (19)$$

Besides giving an approximate conversion of Q and RMR right down to faulted rock (one that does not vanish) it also gives convenient access to Bieniawski, (1989) stand-up time cases as shown in Figure 12. These two figures have general application in drill-and-blast-tunnelling, and are also helpful when assessing stand-up time and support needs in TBM tunnels, where the lack of ready access to the face may greatly increase tunnelling difficulties.

In medium to good quality rock, on either side of the no-support boundary in Figure 11, the need for support in a TBM tunnel is less than in a drill and blast tunnel due to a higher (2 to 5 times higher) assement of the Q-value. This area is cross-hatched for emphasis.

5 TBM TUNNELLING IN JOINTED AND FAULTED ROCK

Two topics that are of extreme importance to successful TBM tunnelling, that are highlighted in papers in this session are:

1. successful prognoses of TBM performance
2. successful tackling of fault zones

Each has a strong impact on safety and on the environment, both inside and sometimes outside the tunnel.

Barla et al. (1999) give a very interesting comparison of three modelling methods applied at a faulted zone in a TBM tunnel, which subsequently delayed the tunnel for a period of 6 to 9 months, due to high pressure inflows, outwash of fines, "church roof" and "natural shaft" formation. (The fault zone modelled by the authors subsequently slowly crossed the tunnel in a sub-parallel manner, affecting progress for more than 50 meters). The Q-value was as low as 0.007 in places, and had disasterous results on progress. Discontinuum modelling, as expected, gave the most realistic results, as shown by the authors.

In addressing the special problems of squeezing ground and fault zones in TBM tunnelling, Schubert et al. 1999, (this session) have demonstrated the potential value of displacement vector monitoring. A "normal" vector of about 10° from vertical

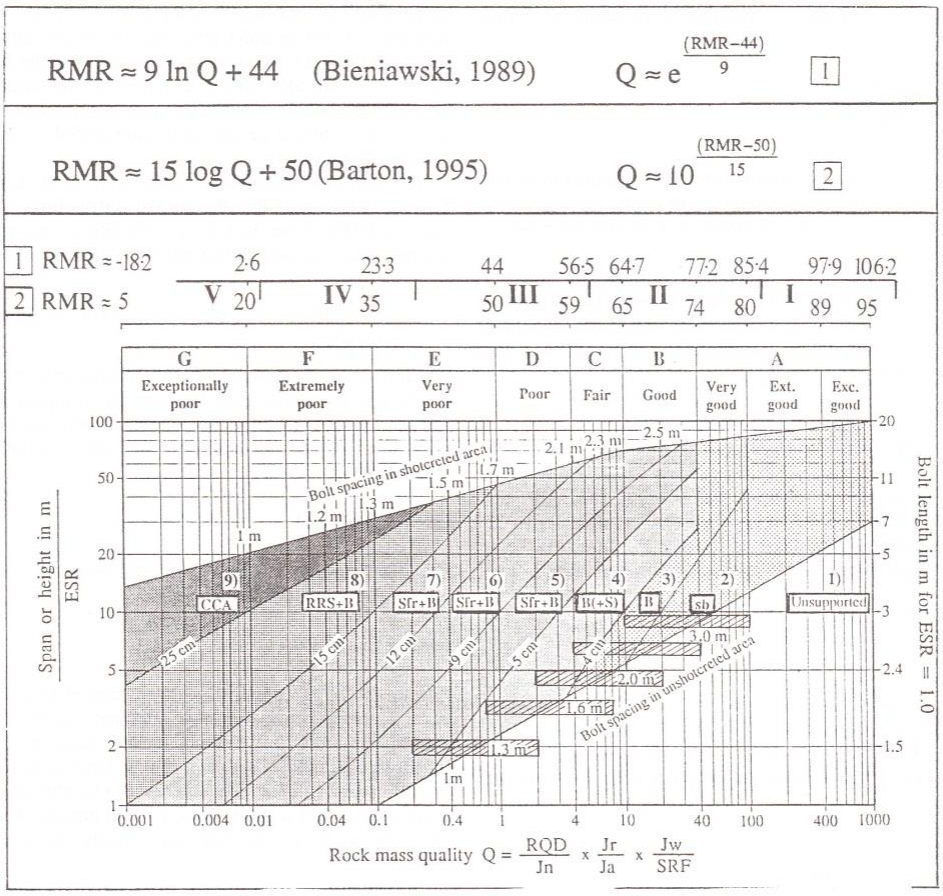

Figure 11. A practical conversion between RMR and Q which does not vanish in faulted rock. Support classes and methods from Grimstad and Barton, 1993.

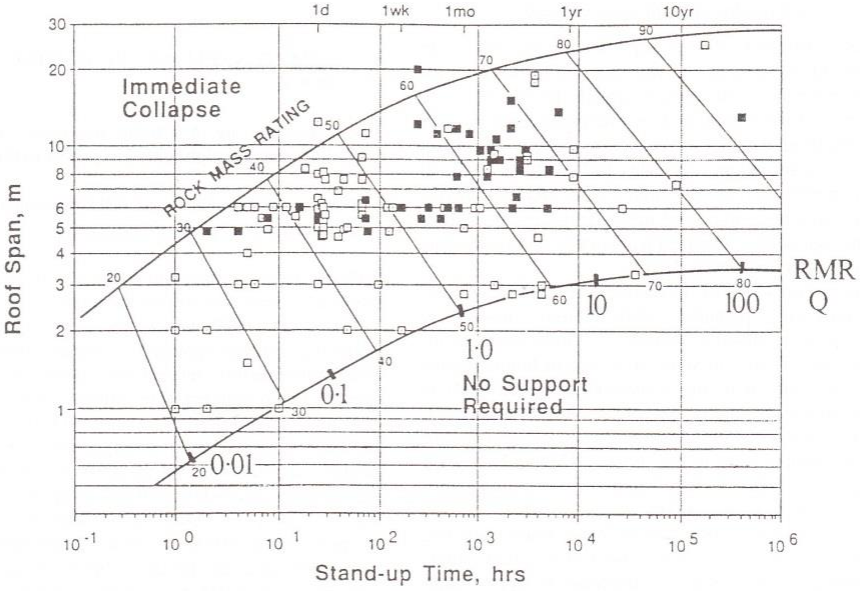

Figure 12. Stand-up time estimate using the RMR- log Q conversion given in Figure 11.

(out from the face) reportedly shows first an increase then a reduction before returning to the pre-fault level after passing through a fault. As pointed out by the authors this method is limited to TBM without shields, and is of course more reliable in conventional tunnelling.

In another paper from Italy, Astolfi et al. (1999) describe two inclined TBM tunnels that were to replace surface penstocks at existing hydropwer stations. They describe a comprehensive suite of preinvestigations and testing, which were easier than at the faulted tunnel described by Barla et al. 1999, due to the much shallower siting of the tunnels. The authors applied RMR and the rock structure rating RSR of Wickham and Teidemann, 1974, to compare predicted and observed conditions. They also show attempted correlations of inverse penetration rate (FPI = cutter load/penetration rate) with RSR $_{TBM}$. The correlation appears to be quite good for one project, but very poor for the second project.

5.1 Q_{TBM} for jointed and faulted rock

These two papers, one on TBM prognoses, and the other on the serious consequences of fault zones in TBM tunnels, provide a good excuse for introducing (after 25 years delay) a parameter called Q_{TBM}. The Q-value alone, as suggested in Figure 13, is insufficient for quantifying penetration rate (PR) and advance rate (AR), without the addition of some rock-cutter interaction parameters like SIGMA/F, shown in Figure 14.

SIGMA is an empirical estimate of rock mass strength that includes Q, σ_c, I_{50}, joint orientation and strength anisotropy, and F is cutter force. CLI is the cutter life index (NTH, 1994), q is the quartz content (%) and σ_θ is the stress on the tunnel face normalized to about 100 m depth. The value of Q_{TBM} may, in exceptional cases, range over twelve orders of magnitude. When below about 10^{-2} or above 10^4, exceptionally slow progress is made. Ideal conditions are seen in Figure 14 when Q_{TBM} is about 0.1 to 10, though tunnel size will be important. Penetration rate (PR) is estimated or back-calculated as follows:

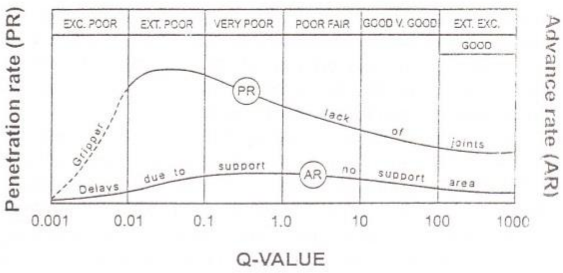

Figure 13. A conceptual relation between Q, PR and AR for TBM tunnelling needs some rock-machine interaction parameters for proper quantification.

$$PR \approx 5Q_{TBM}^{-0.2} \quad (20)$$

$$Q_{TBM} \approx (5/PR)^5 \quad (21)$$

These equations are used for prediction during feasibility studies, and for back-calculation during tunnelling (Barton, 1999b). Actual advance rates are dependent on utilization U, since:

$$AR = U.PR \quad (21)$$

However, an alternative way of expressing this equation is to relate the negative (deceleration) gradient of advance rate (m) to the time period (one shift, one day, one week, one month etc.). In the following equation, T is expressed in hours:

$$U = T^m \quad (22)$$

5.2 Quantifying the unavoidable TBM slow-down experienced with time

Upon reflection, the speed of a TBM through a tunnel resembles

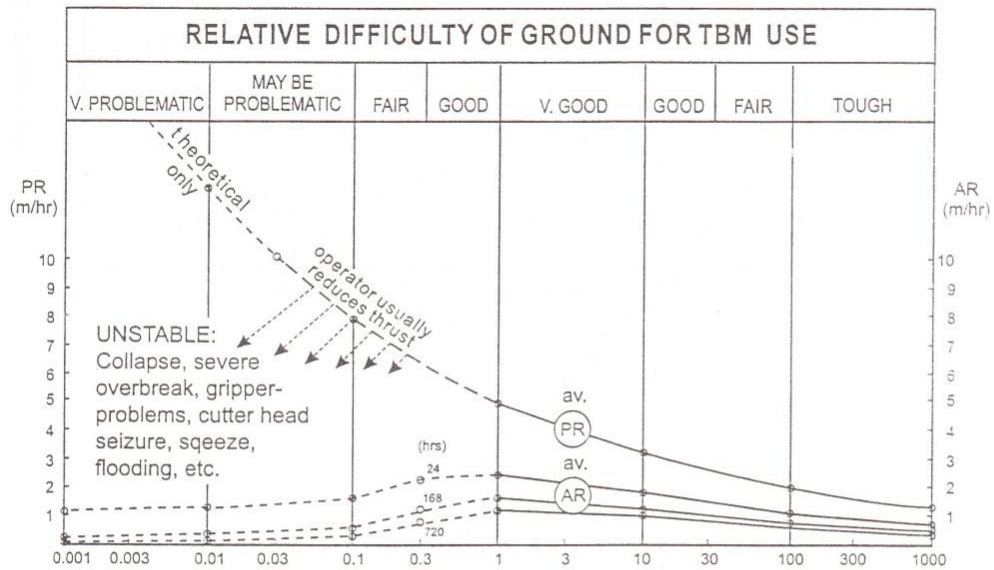

$$Q_{TBM} = \left[\frac{RQD_0}{J_n} \times \frac{J_r}{J_a} \times \frac{J_w}{SRF} \times \frac{SIGMA}{F^{10}/20^9} \times \frac{20}{CLI} \times \frac{q}{20} \times \frac{\sigma_\theta}{5}\right]$$

Figure 14. Suggested relation between PR, AR and Q_{TBM} (See text for explanation of symbols). Barton, 1999b.

life's progress. The longer the life the slower the progress and the greater are the chances for adverse statistics. Nevertheless for short periods, fast progress can still be achieved even near the end of tunnelling. But the machinery gets slowly worn out, and sometimes the main bearing needs replacing.

As in life itself, it is unexpected events that cause the problem, especially if one is too late to prepare ahead of time. TBM tunnelling through a fault zone such as that illustrated in Figure 15 seldom goes smoothly, even with forewarning. Forewarning increases safety and improves the tunnelling environment, and maybe that at the surface. A delay of several months may be reduced to a few weeks, by the investment of a few hours in probe drilling and a few days in pretreatment.

A survey of 145 TBM projects involving more than 1000 km of tunnels (Barton, 2000b) reveals systematic decelerating trends as summarized by the five lines and three curves shown in Figure 16. The major part of most TBM tunnels obviously follow the lines, and on average lie between lines 1 and 3. Some best performances and fantastic world records lie around the "WR" line in Figure 16.

The gradients (m) of these more or less straight lines of average performance, usually vary from about –0.15 to –0.25 when conditions are favourable for TBM tunnelling. The data given by authors Astolfi et al. (1999) for the two steeply inclined TBM tunnels in Italy, (mean PR = 2·5 and 2·6 m/hr, mean daily rates = 11·2 and 12.0 m or AR ≈ 0.55 to 0.60 m/hr) give quite

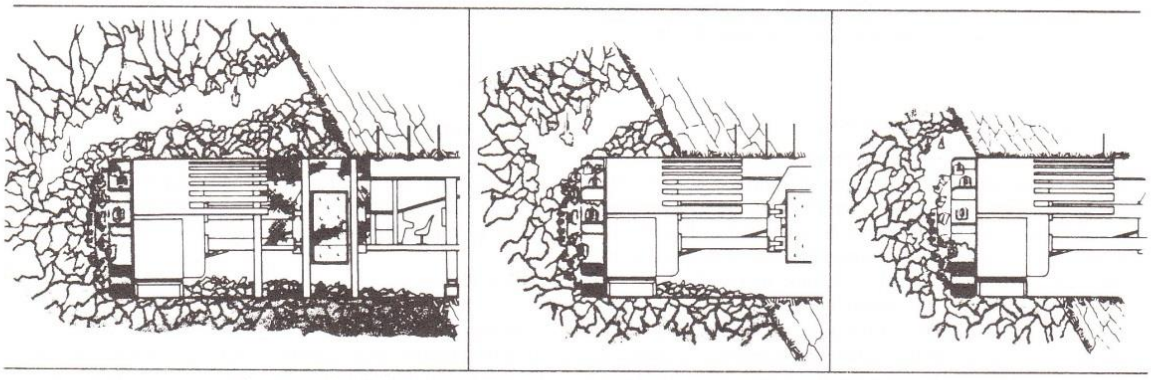

Figure 15. The challenge of faulted rock is still causing big delays in TBM tunnelling and needs quantifying. Robbins, 1982.

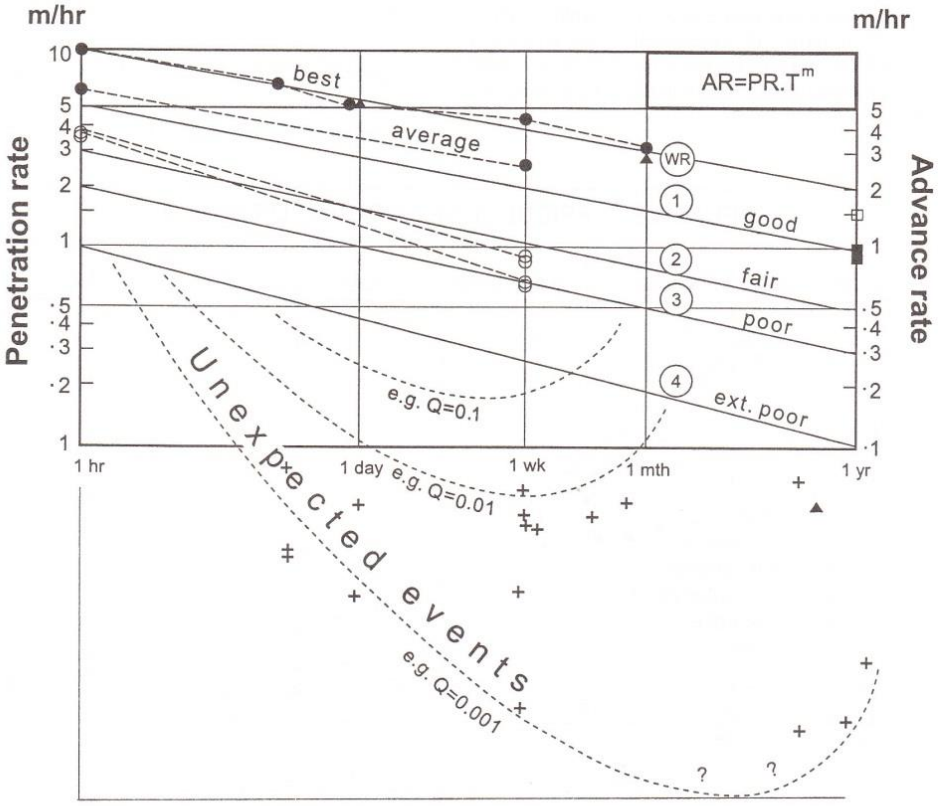

Figure 16. General trends of deceleration from 145 TBM projects consisting of more than 1000 km of tunnels. (Barton, 2000b).

steep deceleration gradients (m) when plotted in Figure 16, confirming the lower utilization achieved in inclined TBM tunnels, as noted by the authors.

"Unexpected events" (shown by the three curves in Figure 16) incur still larger gradients, which may be about –0.5 (for Q ≈ 0.1) –0.7 (for Q ≈ 0.01) and even –0.9 (for Q ≈ 0.001). These are the real problem areas for TBM tunnellers that need to be solved in the next century, with better methods of pre-investigation, probe drilling, remote sensing and last but definitely not least; successful pre-treatment. Safety, cost and environmental impact are each critical here, as illustrated too many times in TBM projects.

5.3 The constant problem of fault zones in TBM and other tunnels

At the start of this paper, dilation (or the lack of it) was mentioned as potentially "the most important parameter" in rock engineering. A tunnelling or mining engineer's working day is turned up side down by the least dilatant feature of all –the fault zone, where outwash of fines or overbreak, or loss of material through squeezing complicates progress very much in all types of tunnelling, but especially in TBM tunnelling.

The dramatic slow-down of progress seen under "unexpected events" in Figure 16 may delay progress for weeks, months, even years, and occasionally permanently. Even top-of-the-line machines as used at Pinglin in Taiwan, may fail, due to the difficulty of improving the rockmass and rock hydraulic qualities in major fault zones. Safety and environmental aspects may dominate as delays increase due to huge inflows. In Kashmir, more than 20,000,000 m^3 of water has flowed into a TBM tunnel since 1993. Initial pressures may have been 10 MPa or more. (Barton 2000 b). Villagers and farm animals have lost their water supplies as surface streams and wells have disappeared.

The time delay problem is actually "simple" to understand because of the over-riding influence of the gradient (m). For a tunnel section of length L, (or fault width L in the tunnelling direction) we can derive the following simple equation:

$$T = (L/PR)^{\frac{1}{1+m}} \qquad (23)$$

(T = hours, L = meters, PR = m/hr, m is negative)

When L (in meters) is numerically larger than PR; for example 15 meters compared to 2 m/hr, the quotient is larger than unity (i.e. 7·5 in this case) and a large negative value of m (such as -0·7 for Q ≈ 0.01) will result in a predicted fault penetration time of more than 800 hours.

In practice it is usually impossible to progress at a uniform rate through an untreated fault zone. Cutterhead blockage, void formation and many other safety and environmental hazards prevent progress until the Q-value is raised (by grouting and other artificial measures). This will help the gradient (m) to become less steep.

This brings us to the important subject of grouting, which is vital under our dams and in the tunnelling and mining industries in general. The environment both inside and outside our tunnels and shallow mines is greatly affected by the success or failure of pre-grouting, or by the frequently great difficulties of post-grouting.

6 GROUTING OF JOINTED ROCK

Two papers on grouting have been presented in this session of the Congress. Both come from Sweden, but clearly one of our leaking Norwegian tunnels has been a useful proving ground in the case of the polyurethane grout described by Andersson, (1999). Reaction with water to produce CO_2 to give an important foaming action prior to stiffering has proved to be useful for controlling concentrated leakages, even in the case of post-injection.

The Norwegian tunnel in question suffered from insufficient pre-investigations ("the lowest bidder syndrome") and large inflows, a drained lake, damage to local forest areas, and settlement damage to housing nearly half a kilometer away. Rock stress measurements, permeability testing and variously oriented refraction seismic surveys should have been performed, due to the strong linkages that are often found between common trends of stress, structure, velocity and permeability, and their frequent, anisotropy, (e.g. Barton, 2000a).

In the case of tunnelling, and especially TBM tunnelling, the frequent presence of high inflows in the neighbourhood of erodable material, suggest that probe drilling and appropriate use of polyurethane and microcements in pre-injection fans will give a marked improvement in tunnel stability, deformation and the resulting inflows that are experienced. The interaction between these three factors is obviously important. When these three factors are controlled, continued good TBM progress is often assured:

6.1 Improvement of rock mass properties with pre-grouting

We can utilize parameters in the Q-system as a preliminary demonstration of what might be achieved when performing pre-grouting ahead of a tunnel to prevent damage to the environment. Due to easier penetration of the most permeable joints and channels, (frequently those parallel to the major stress), there may be significant rotation of the permeability tensor and reduction in its magnitude, (Quadros and Filho, 1995). If some cement-rock bonding or cohesive strength development is involved, then we may expect the following possibilities in an imaginary but not too optimistic case.

effective RQD	increases	e.g.	30 to 50%	
effective J_n	reduces	e.g.	9 to 6	
J_r	increases	e.g.	1 to 2	(changed set)*
J_a	reduces	e.g.	2 to 1	(changed set)*
J_w	increases	e.g.	0.5 to 0.66	(perhaps Jw = 1 is achieved)

SRF would reduce only near surface e.g. 2.5 to 1

(* it may be appropriate to qualify with the word "perhaps" in several cases here)

Before pre-grouting $Q \approx \frac{30}{9} x \frac{1}{2} x \frac{0.5}{2,5}$

≈ 0.3

After pre-grouting $Q \approx \frac{50}{6} x \frac{2}{1} x \frac{0.66}{1 or 2.5}$

≈ 11 (or 4·4)

When tunnelling through the grouted zone, if the couplings between Q, V_p, M, L, P_r and Δ shown in Figures 7, 9 and 10 are believed, several improvements will be experienced due to the pre-grouting. For the sake of this demonstration, porosity n = 1% and uniaxial compression strength σ_c = 100 MPa will be assumed, and a 10 m span tunnel will be utilized.

Before pre-grouting	*After pre-grouting*	*(alternative)*
Q ≈ 0.3	Q ≈ 11	(Q ≈ 4·4)
V_p ≈ 3.0 km/sec	Vp ≈ 4.5 km/sec	(V_p ≈ 4·1) km/sec
L ≈ 3 ($3x10^{-7}$ m/s	L ≈ 0·1 (10^{-8} m/s)	(L ≈ 0·2) 2 x 10^{-8} m/s
M ≈ 7 GPa	M ≈ 22 GPa	(M ≈ 16) GPa
P_r ≈14 tnf/m^2	Pr ≈4·5 tnf/m^2	(P_r ≈ 6·1) tnf/m^2
Δ ≈ 33 mm	Δ ≈ 0·9 mm	(Δ ≈ 2·3) mm

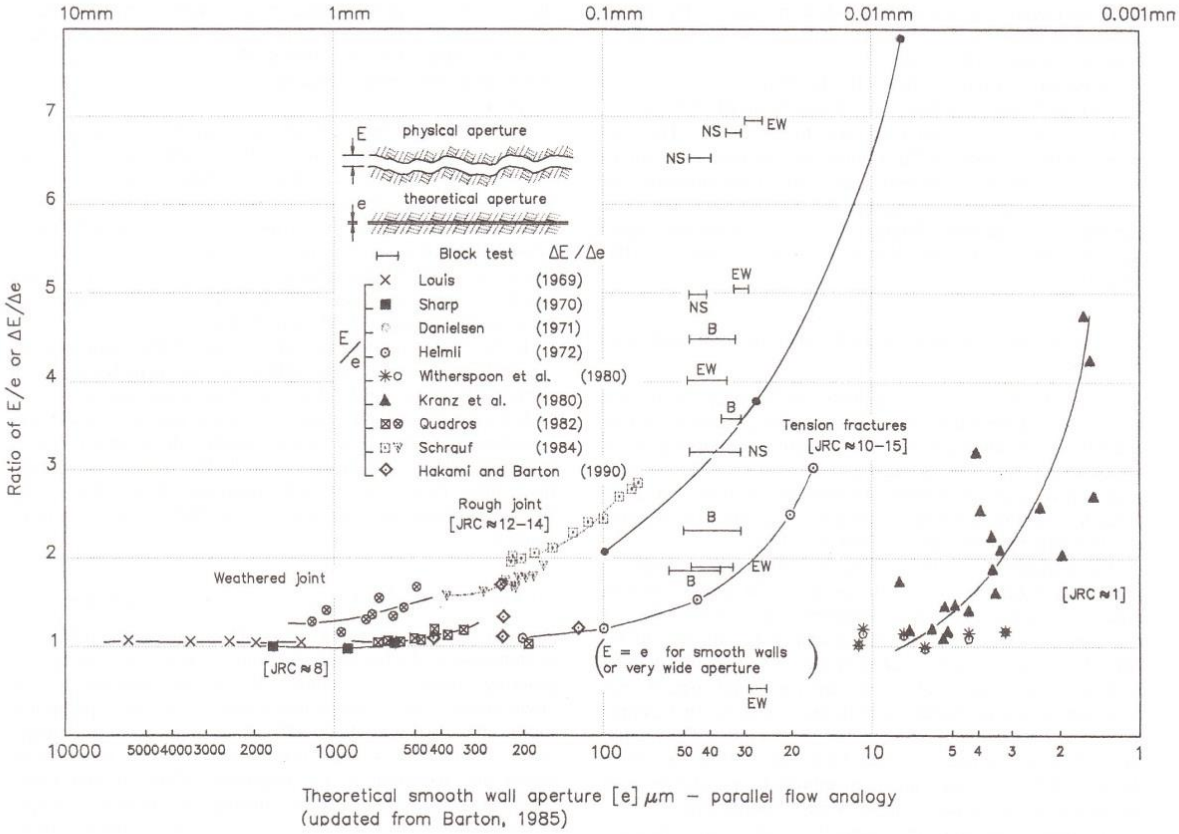

Figure 17a. Mismatch of the apertures E (physical) and e (hydraulic) in flow-closure and flow-shear tests. Barton and Quadros 1997.

Perhaps these improvements appear too great? Nevertheless rock masses that are in need of pre-treatment such as a "very poor quality" Q = 0.3 rock mass, do experience a marked reduction in support needs and may be temporarily self-bearing. In the above case, Figure 11 informs us that the permanent support needs might change as follows:

Without pre-grouting	*With pre-grouting*	*(alternative)*
B 1·5 m/sec	B 2·4 m c/c	B 2·1 m c/c
S (fr) 12 cm	S (fr) 4 cm	S (fr) 5 cm

6.2 *Channels and joints*

In the second Swedish paper on grouting, Eriksson et al. (1999), introduce some theoretical grout take models for injection from boreholes. One of these includes allowance for channel apertures and parallel plate hydraulic apertures. The authors also make use of the ratio E/e between the mean physical joint aperture and the theoretical smooth wall hydraulic aperture respectively. This ratio is essential when assessing groutability with particulate grouts. Some key sets of test data for E/e are presented in Figure 17a, b and c.

Figure 17a is an updated assembly of mostly normal stress-flow test data, but with one set of "vertical" data marked "EW" and "NS" that involved slight shearing in an in situ block test, (Barton et al. 1985). Esaki et al. 1995, in Figure 17b, also show "vertical" shear data that cross the JRC curves suggested by Barton et al. 1985 for closure-flow modelling. Finally in Figure 17c there is another set of coupled shear-flow data from recent work by Olsson (1998), that also crosses the normal closure curves marked with JRC_o, (the subscript refers to nominal lab-scale sample sizes i.e. L = 100 mm).

A working approximation for the normal closure-flow data that is built into the Barton - Bandis joint model, demonstrates the very strong influence of roughness, due to the inter-locking asperities, tortuous flow paths, and areas of contact or near contact:

$$e \approx E^2/JRC_o^{2.5} \qquad (24)$$

The recent work of Olsson (1998) shown in 17c and the other

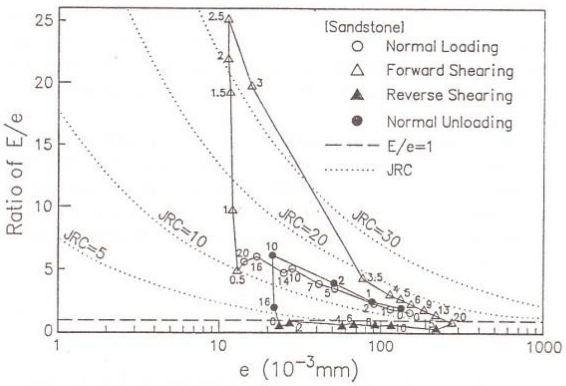

Figure 17b Mismatch of the apertures E (physical) and e (hydraulic) in flow-closure and flow-shear tests. Esaki et al., 1995.

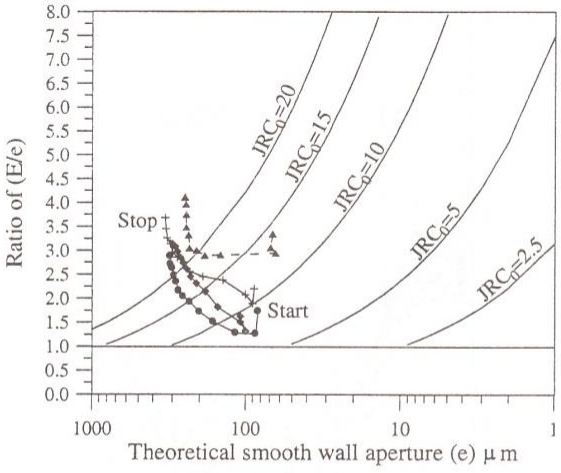

Figure 17c Mismatch of the apertures E (physical) and e (hydraulic) in flow-shear tests. Olsson 1998.

sets of "vertical" shear-flow data that obstinately cross the JRC-labelled curves (as if roughness was increasing with shear which is clearly untrue) has stimulated the development of a set of complementary "mirror image" curves which follow the steeply inclined (so-called "vertical") shear flow data. The simple relationship that was needed to achieve this is as follows (Olsson and Barton, 1999):

$$e \approx E^{1/2} JRC_{mob} \qquad (25)$$

Here JRC_{mob} represents the mobilized roughness as used in the Barton – Bandis joint model. It is suggested that equation 24 can be used for both closure-flow and for minor amounts of shear ($\leq 0.75\ \delta_{peak}$) while equation 25 should be used for shear displacements $\geq \delta_{peak}$, in other words for asperity damage and gouge production. These causes a rapid increase in E/e despite the large, dilation-related aperture E.

These details of joint behaviour may appear too detailed for a General Report. However they are very important for improving general coupled M-H flow modelling and for estimating groutability when particulate grouts are involved. Both these subjects are of fundamental importance to improved understanding, improved design, and improved practice in rock engineering. Obviously their effect on the environment, both inside and especially outside a tunnel, are fundamental.

The subject of this sub-section "channels and joints" is designed to stimulate discussion of these two features, both as regards their variable occurrence in drill-and-blast and TBM tunnels (which are real and three-dimensional) and in their theoretical appearance in two-dimensional simulations, such as the distinct element and analytical explorations of shearing phenomera shown in Figure 18.

These simulations by Shen, (Shen and Barton, 1997) show a general tendency for shearing at approximately the 45° positions, when vertical and horizontal stresses are acting on simulated tunnels. In the cases illustrated, strong stress anisotropy (σ_h/σ_v = 0.25) was used to emphasise the effect. This shearing will have the tendency to generate channels at block corners in the third dimension, while dilation-enhanced joint apertures may be expected to enhance (i.e. worsen) leakage into the tunnels. Obviously, strongly anisotropic joint structures will modify the trends shown.

When observing leaking joints in TBM tunnels, it is often easier than in drill-and-blast-tunnels to see that a whole joint

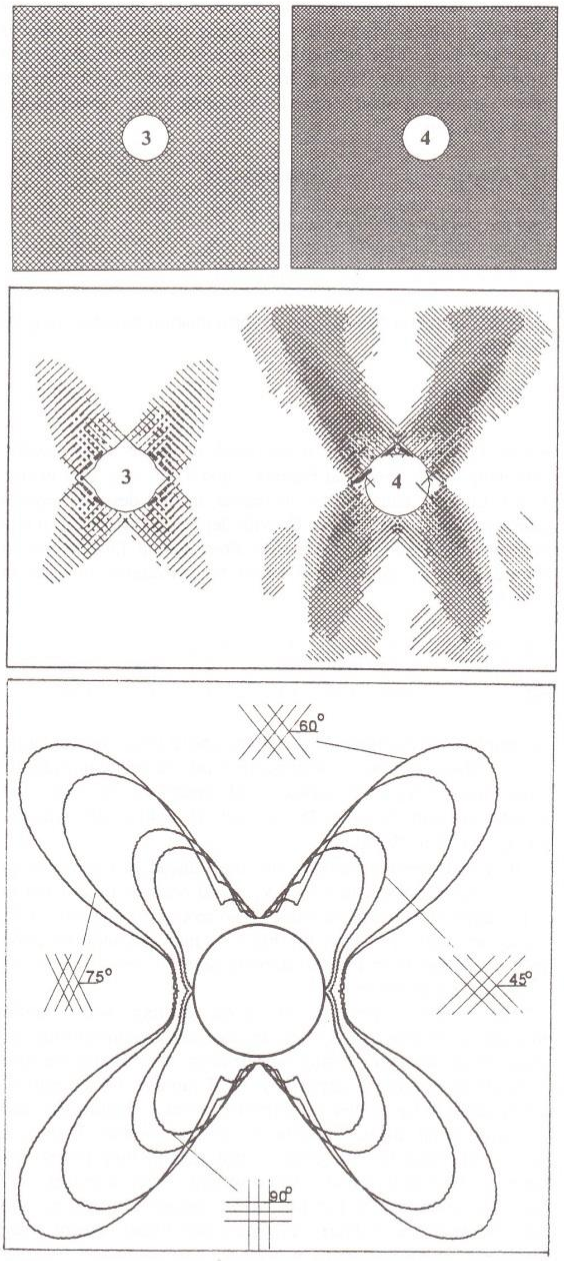

Figure 18. Zones of joint shearing from two distinct element UDEC models and from analytical Mohr Coulomb formulations. Shen and Barton, 1997.

plane may be involved, due to continuous rust staining and "uniformly" wet tunnel walls below the joint. Nevertheless there may be jets of water appearing from channels within the same joint plane, channels that are in-plane rather than the third-dimensional block-corner channels as seen so easily in our numerical "slices" (Figure 18).

6.3 Grouting and Lugeon testing

Another factor to be considered when assessing groutability, is

whether injection pressures will be higher than those used in, for example, Lugeon tests where an excess pressure of 1 MPa is generally used. If the answer is yes one may theoretically expect a better groutability, at least from the permeable joints that are most easily jacked open. Recalling the lower-bound approximation:

$L \approx 1/Q_c$ (equation 10)

and the seismic velocity relation:

$V_p \approx 3{\cdot}5 + \log Q_c$ (equation 8)

we may suggest a lower-bound approximation between Lugeon value and Vp:

$$L \approx 10^{(3{\cdot}5-Vp)} \qquad (26)$$

Since V_p increases with stress level or depth (i.e. roughly following trends shown in Figures 7 and 9) we may also expect lower Lugeon values with increased depth, despite perhaps unchanged rock quality Q or Q_c with depth. The trends from this equation, as shown from the two French dam foundations in Figure 8 are as follows and might be considered realistic in principle:

Vp km/sec	6.5	5.5	4.5	3.5	2.5	1.5	0.5
L (Lugeon)	0.001	0.01	0.1	1	10	100	1000
(Q_c	1000	100	10	1	0.1	0. 01	0.001)

As emphasised in Figures 7 and 9, the above tentative tabulation of Q_c values will be misleading if depth varies. For example from Figure 7, V_p = 5.5 km/sec could apparently imply $Q_c \approx 0.4$ at 1000 m depth, $Q_c \approx 4$ at 750 m depth, $Q_c \approx 40$ at 100 m depth, and $Q_c \approx 100$ at 25 m depth.

If remote sensing methods are used ahead of tunnels or in mines, this stress sensitivity of V_p could perhaps be utilized in expectation of low Lugeon values (and reduce groutability) if V_p values are high. However the high V_p may not indicate good rock conditions from a tunnel stability point of view, since the Q or Q_c value may not be high.

The potential benefits of probe drilling with careful monitoring of penetration rates, and occasional core drilling are clear. When injection testing (and leakage monitoring) are also used ahead of tunnels (especially TBM tunnels) on a "routine-when-needed" basis, then "unexpected events" (Figure 16), and "environmental impacts" can be reduced in number. There is a very strong need for improved control of tunnelling projects as we enter the next century, when general water stortages may force acceptance of the fact that tunnel leakage is a wasting of a valuable resource. Polyurethane foam and micro cements may perhaps be environmentally acceptable barriers to this leakage, when applied in an approved and systematic manner.

7 DISCOUNTINUUM MODELLING AND ANISOTROPY

In the last section of this General Report, efforts will be made to reinforce some of the discussion that was presented earlier. In section 3, *Input data and Constitutive Models,* questions were raised as to the whether it was defensible to ignore the frequently anisotropic patterns of jointing when performing continuum models. A related question was whether it was defensible to ignore the effects of high stress anisotropy on the magnitudes of input parameters. I concluded that most rock masses and boundary conditions should disqualify the use of isotropic continuum modelling and associated equal-in-all-directions input data. In bedded strata the use of transversely isotropic

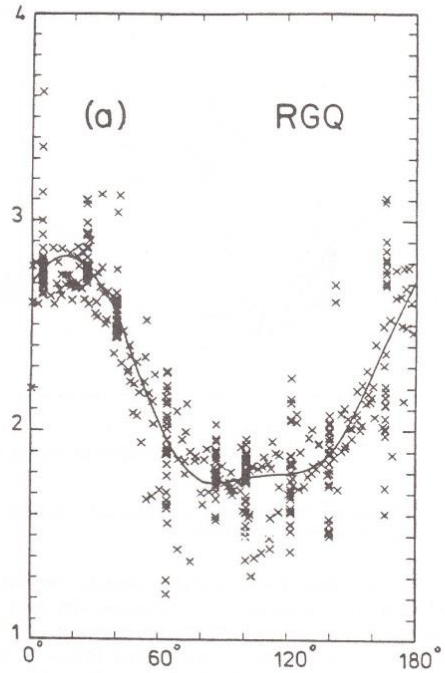

Figure 19a. Anisotropy of V_p due to dominant jointing. Nunn et al. 1983.

parameters, or occasional orthotropic distributions of input data may add some degree of realism to the continuum models. Likewize , ubiquitous joint formulation as in FLAC and FLAC^{3D} help to give a degree of reality to the continuum modelling.

7.1 Anisotropic input data

The problem of anisotropy is emphasised by an interesting article on the anisotropic behaviour of jointed rock masses around caverns, given by Hibino and Motojima, (1999) in this session. The authors have observed how in situ test data such as deformation modulus and shear strength may become strongly anisotropic (i.e. ratios > 2 to 1) even when joint frequency dominates by only 10% in a particular direction. Measured deformations at caverns indicated a stronger effect from joint anisotropy than from stress anisotropy according to the authors.

The effect of stress anisotropy, or joint anisotropy, or their combined effect when these anisotropies are nearly coaxial, can be measured by seismic surveys. Near the surface, refraction seismic can be used, as illustrated by data from Nunn et al., 1983 and Oda et al., 1986 in Figures 19a and 19b.

A V_p anisotropy as much as 0.5 to 1 km/sec implies a significant modulus anisotropy, which can be estimated from an equation appearing in Figure 7. The units of M are GPa, and V_p is expressed as km/sec.

$$M \approx 10.10^{\left(\frac{V_p-3.5}{3}\right)} \qquad (27)$$

For example an anisotropy similar to that shown in Figure 19a (from Nunn et al., 1983) would give the following estimates of modulus anisotropy:

Case a (approx.) V_p = 2 km/sec $M \approx 3.2$ GPa
V_p = 3 km/sec $M \approx 6.8$ GPa

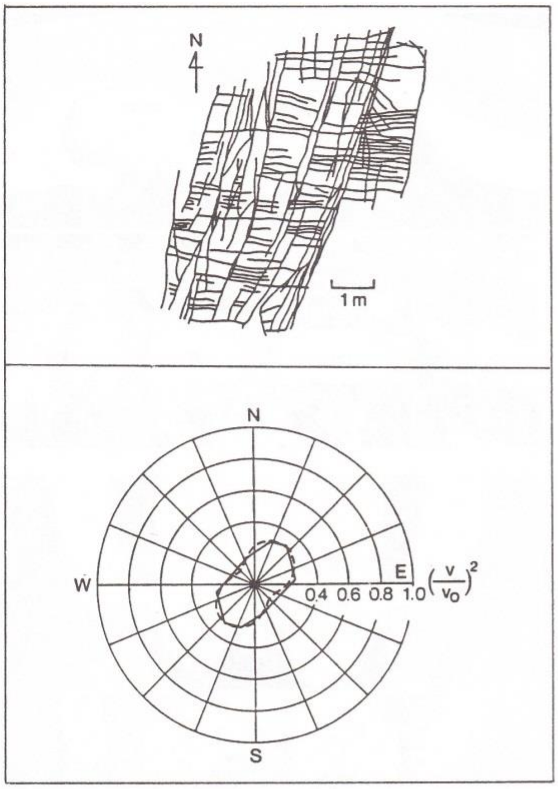

Figure 19b Velocity reduction effect of heavy jointing. Oda et al., 1986.

Since the cases reported by Nunn et al., 1983 were actually limestone, corrections would also be needed for n% and σ_c and perhaps depth, if this was different from the nominal shallow refraction seismic depth of 25 m, which is the basis for equations 8 and 27.

7.2 A discussion of discontinuum modelling

There are some fine examples of the use of the discontinuum modelling in session 1 of this Congress, and some e.g., Barla et al., (1999) and Hakala et al., (1999) have been referred to already. To these references we can add the interesting bridge pier investigations using 3DEC, reported by Alfonsi et al., (1999), in which some failure modes were investigated, and the slope stability and slope failure mode investigations reported by Zettler et al., (1999) and Sjöberg, (1999), using mostly UDEC.

An elegant and early demonstration of the power of discontinuum modelling, following Cundall's pioneering work in the late sixties and seventies, is the slope failure mode demonstrations shown in Figure 20. To some, the continued use of continuum modelling in rock mechanics is surprising when tools such as UDEC, 3DEC and DDA are now available.

Choice of modelling technique should depend on the degree of jointing (or lack of jointing) as the case may be. We may expect greatest applicability of discontinuum codes such as UDEC, 3DEC or DDA in a central band of rock qualities, as illustrated schematically in Figure 21. The suggested range of values of Q between 0.1 and 100 corresponds to RMR values from roughly 30 to 80. When anisotropic jointing is present, or when dominant joints sets are not parallel or perpendicular to principal stresses, there will be a particular need for

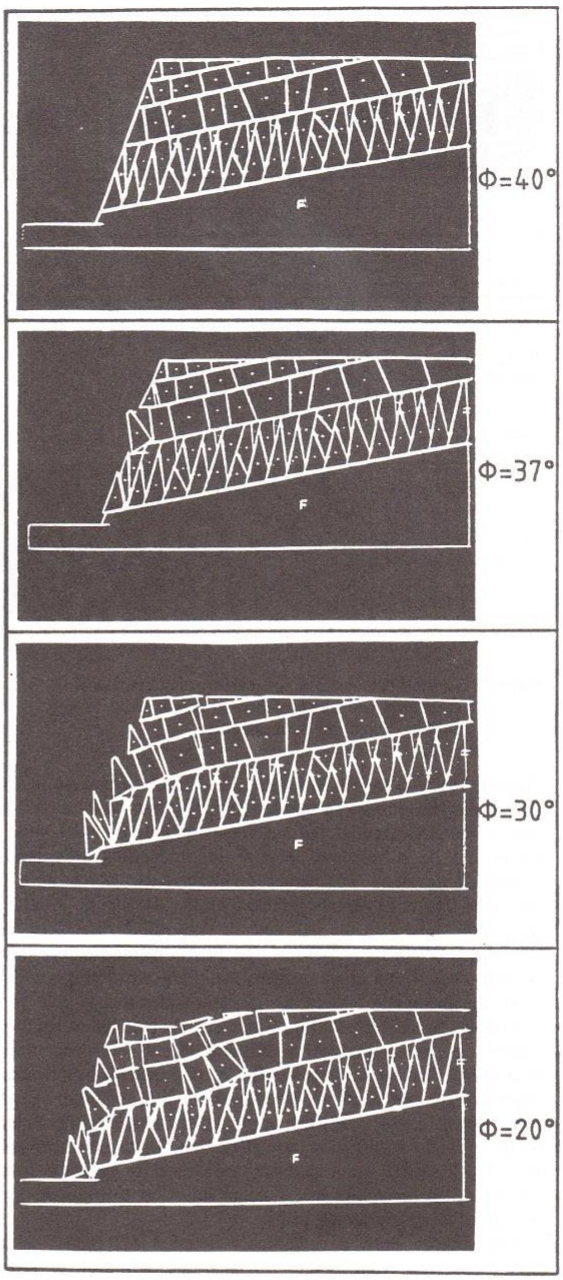

Figure 20. An early demonstration of the power of discontinuum modelling, using the rigid block method. (Cundall et al., 1977).

discontinuum modelling. Even the "sedimentary rock" example in Figure 21 may give strong joint-related responses to excavation with shearing in the neighbourhood of the four "corners", like in Figure 18, together with bending or cantilevering of the strata in the arch.

When comparing the results of continuum and discontinuum models of the same engineering structure, such as done for a faulted TBM tunnel by Barla et al., (1999), the difference in levels of information that can be gleaned from the different models is often spectacular. An example by an NGI colleague,

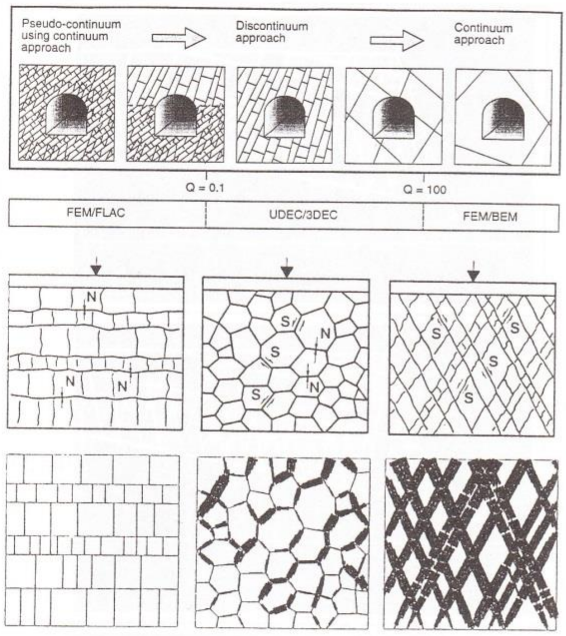

Figure 21. Approximate range of applicability of discontinuum modelling, and details of three models showing various degrees of joint shearing response.

(Backer, 1995) is shown in Figure 22. A zone of tension in the arch of the two motorway tunnels (the third is a ramp tunnel) is seen in the UDEC model, but not in the continuum model, which would not be a relevant method for modelling this joint-dominated problem. The larger displacements, which have a trajectory that is obviously affected by the dominant jointing, are clearly missed in the isotropic model, which resembles "a-hole-in-rubber" in its responses. The FLAC method comes into its own where large displacements are involved, through over-stress, squeezing and flow of incompetent material.

Coupled process modelling, which strictly belongs in another session, is an important sophistication of "applied rock mechanics", and there are a handful of fine articles in this area which deserve mention here. Dershowitz et al., (1999) have used their discrete fracture network approach for studying thermally assisted gravity segregation, so-called TAGS, for enhanced oil recovery. Preferred joint pathways are used to enhance heat transfer in oil reservoirs using steam injection to improve the flow of oil to the producing wells.

The authors show a remarkably detailed 3D model of a jointed reservoir from Texas. However the definition of joint aperture (1/2000 of model thickness, without response to effective stresses) is simple, due to the size and type of model used. The authors use a novel "hot particle" conductive heat transport, together with conventional conductive heat transport using standard diffusion modelling.

A nice contrast to this complex but rigid 3D fracture network, is the simple demonstration model of coupled hydro-thermo-mechanical behaviour, given by Gutierrez and Makurat, 1997. The upper pair of diagrams in Figure 23, show oil-water saturation levels and temperatures after 150 days of cold water flow into a central borehole, in the case of an uncoupled model. In the lower pair of diagrams, an uncoupled model (a) shows less oil left in place than the coupled model (b), due to contraction of the matrix and increased aperture of the joints due to the cold water.

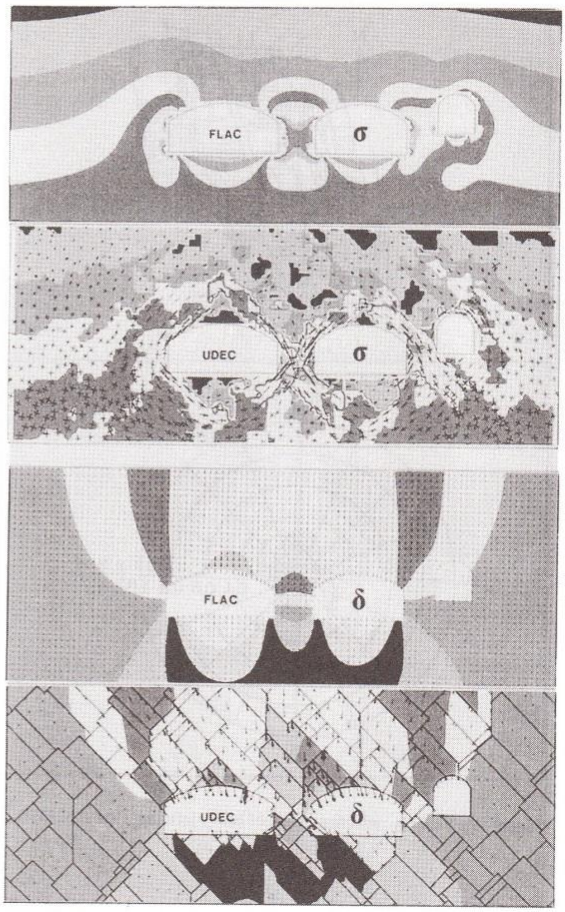

Figure 22. A comparison of information from continuum and discontinuum models. The UDEC-BB model has systematic bolting, based on Q-values. Backer, NGI, 1995.

These authors used a one-way coupling between PROFHET (NGI, 1992) for calculating fluid pressure, temperature and two phase (oil/water) flow, and the UDEC-BB code for updating the joint aperture changes caused by effective stress and temperature changes.

A goal for the next century, with the help of ever-improved computing power, will be the ability to run a fully coupled HMT model with non-linear properties with a complex 3D joint network model such as FRACMAN, NAPSAC or 3DEC. Definition of the void space in 3DEC (for fluid flow calculation) and incorporation of a non-linear joint model could be the best way to achieve this in rock mechanics.

The modelling reported by Damjanac et al., (1999) to this session, highlights some of the challenges that will be involved in future 3D fully coupled HMT modelling. They describe the thermo-mechanical response to heating of jointed tuff by simulating a drift scale heater test at Yucca Mountain, Nevada, USA. They use an unconventional, numerical method for developing joint behaviour for the UDEC models. Whether their extreme dilation angles are realistic needs to be discussed. However, studies by Cundall have shown good correlation between particle flow code PFC representation of rough joints and the rough end of the JRC scale, (Cundall, 1996).

Li and Roegiers, 1999, highlight the coupled nature of the real processes that are probably involved in wellbore stability in

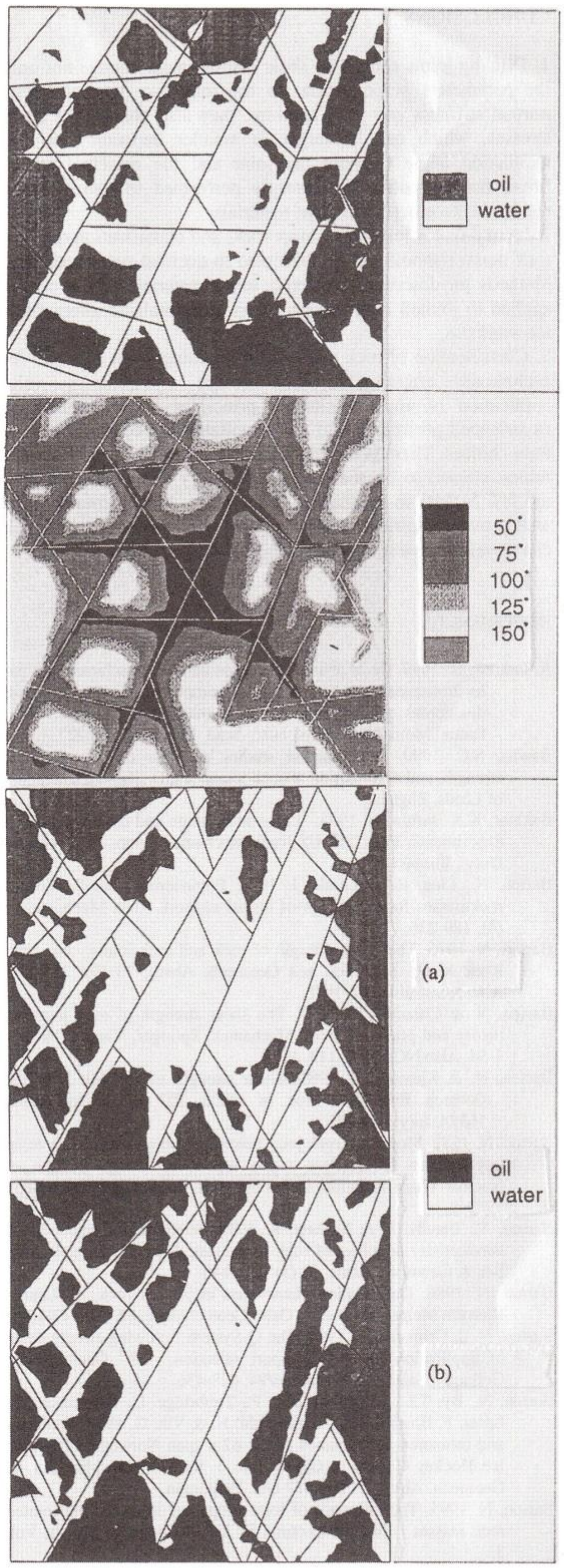

Figure 23. Cold water injection into a jointed hydrocarbon reservoir. The uncoupled model (a) shows less oil in place than the coupled model (b). Gutierrez and Makurat, 1997.

shales. A recently developed fully coupled thermoporoelastic model is used by the authors to demonstrate the various effects of cooling and heating on borehole failure modes. The fully coupled effects of temperature changes on pore pressures are used to explain some of the potential reasons for the great predominance of time-delayed wellbore instabilities in shale. These are important findings, and emphasise, as does Figure 23, the importance of coupled modelling in our applied rock mechanics, whether these are continuum models where relevant or discontinuum models.

8 DISCUSSION

"Applied rock mechanics" is a major theme of our subject, and like a fishnet trawled deep and far, it has bought a wealth of papers and subjects to the surface. The two General Reporters have faced an impossible task, and to all those not referenced, our apologies for lack of space and time. Many more papers of merit, and the General Reporter's referenced ones, are of course in the proceedings, (Volume 1) and were given as Posters during the Congress.

The wide range of topics presented in session 1 can be judged by the following groups of topics in the papers received by the organisers: joints and rock masses, tunnels, caverns, mines, storage, petroleum reservoirs, foundations, slopes, environment, modelling, miscellaneous.

This General Report has therefore focussed on general methods of applied rock mechanics that have potential application in all these fields. An attempt has also been made to focus on useful techniques (and some less useful ones) that we have been using during the 20th century, emphasising where some changes and improvements may need to be made as we proceed to the beginning of the next millennium. Inevitably, and perhaps correctly, the personal bias and individual experiences of the Reporter is easily seen in the treatment of the topics that form each chapter heading:

- Principal stress transformation to joint and failure planes
- Input data and constitutive models
- Classification methods for estimating rock mass properties
- TBM tunnelling in jointed and faulted rock
- Grouting of jointed rock
- Discontinuum modelling and anisotropy

The stress transformation methods of Mohr, (1882) that the civil and geotechnical communities have applied for so many years apparently need reassessment by all geotechnical disciplines working with dilatant materials, such as rock joints, sands, gravels, rockfill and over-consolidated clay. As discussed previously, many have adjusted normal stresses and stiffnesses when dilation occurs, and we have also allowed for changed joint apertures in our stiff material – jointed rock. The adjustment of *shear stresses* when dilation occurs also needs to be addressed in the future. A need for some basic research using laboratory and field tests is apparent, followed by some adjustment of constitutive laws and/or stress transformation routines.

Our papers, conferences and congresses are containing more and more tabulations of input data, often given to several decimal places of false accuracy, to introduce what may be a questionable constitutive model. It is the opinion of this reporter that we may not be following a logical path in rock engineering. Leonardo da Vinci, (in the fifteenth century), Amontons, (1699) and Coulomb, (1773) presented simple theories for friction and cohesion in relation to early machinery and to architecture. The bending, shear and tensile strengths of "white rock" (presumably marble) were apparently reported by Coulomb.

While the cohesive nature of intact rock, until it fails, is unquestioned, it must surely be admitted that only rock joints that are healed display real cohesion. The much used linear Mohr-Coulomb envelope is a mathematical convenience, but also a source of error in our subject. At low stress levels, strength will be over-estimated, at high stress levels it will be under-estimated.

Our tunnels, stopes and slopes usually fail due to unloading or over-loading of a cohesionless, jointed, frictional material. Is it logical to base rock mass shear strength estimates on methods that are more relevant to homogeneous, isotropic materials? Discontinuum modelling, something approaching the real world, conveniently avoids this dilemma.

Classification methods that provide a "number" have been popular in rock engineering for at least the last 30 years. There appears to be a fairly widespread use of RQD, RMR and Q, but inevitably there is misuse, critique and a certain income for lawyers. Has the development been worthwile? In this General Report, the potential uses of Q parameters and Q-values in applying rock mechanics and rock joint principles has been demonstrated to the partial satisfaction of the writer, while the reader may remain to be convinced. Some consider classification to be a switching-off of rock mechanics principles. To those I would suggest that use of the Q-system is definitely not "switching-off". In fact it cannot be applied correctly without thinking deeply about the potential failure mechanism. The process of selecting J_n, J_r, J_a and SRF is actually more applied rock mechanics, than classification.

Common sense allows humans to have a flexible attitude to a wide range of problems, and experts can respond creatively to situations not previously encountered, and learn from experience. When reinforced with the Q-system, which is a form of expert system, the chances of error are reduced since the Q-system does not forget or get tired (paraphrased from Loetscher, 1999).

The various rock mechanics and geophysical parameters that can be related so simply to the Q-value, suggests that a form of *limit state* is captured in the physics of Q (block size x friction coefficient x stress/strength ratio). When Q (or RMR) are truncated, some of the value of each system is compromised, and some fundamental relationships cannot apply.

Tunnelling with capital intensive TBM machines, which can sometimes race at well over 100 m per day or occasionally stall for years, is obviously in need of more attention by geophysicists, by geologists, and by hydrogeologists. Seriously faulted rock was shown empirically (and semi-analytically) to need quality (i.e. Q-value) improvement by grouting and probably by drainage, to avoid almost infinite delays. Since the situation depicted in Figure 15 is already "too late", serious faults must be found and pre-treated, or avoided where possible. This is truly a challenge for the future.

The strongest message that should emerge from this review of numerous applied rock mechanics topics is to view rock masses as discontinuous, and describe them and model them with discontinuum based methods, not modified continuum methods. When a rock mass is not modelled with each of its component parts, a false "black-box" situation arises, and these practitioners will have less and less understanding of the possible real modes of behaviour. Of course when modelling highly stressed massive rock or very small structures such as boreholes, or fully degraded materials, the initially intact or homogeneous state is not in question, and continuum methods can be used with more confidence.

CONCLUSIONS

1. Dilating joints caused by shear displacement change not only the parameters perpendicular to the joint like normal stress, normal stiffness and joint aperture, they also change the shear stresses, which can be larger or smaller depending on the inclination angle between the joint and the principal stress. Stress transformation as currently performed following Mohr theory, is incorrect for dilatant materials.
2. Input data for joints and intact rock, and classification data for rock masses should not be presented to decimal point accuracy. Methods for describing isotropic, intact materials should not be applied to jointed rock masses when more realistic alternatives are available.
3. Classification of rock masses for obtaining input data and for preliminary empirically based design represents a valid application of rock mechanics principles when applied by experienced personnel who are visualizing the consequences of their choices. There is too much excavation world-wide (tunnels, mines, slopes) to be analysed theoretically or numerically, and too few experts to make good judgements. A well founded and well proved empirical method applied by experienced personell can therefore give some consistency of judgement.

REFERENCES

Amontons, G. 1699. De la résistance causée dans les machines, tant par les frottements des parties qui les composent que par la roideur des cordes qu'on y employe, et la manière de calculer l'un et l'autre, Mém. Math. Phys. Hist. Acad. Roy. Sci., 206-227.

Bandis, S.C. 1980. Experimental studies of scale effects on shear strength, and deformation of rock joints. Ph.D. Theses, University of Leeds, England.

Bakhtar, K.& Barton, N. 1984. Large scale static and dynamic friction experiments. Proc. 25th US Rock Mechanics Symp. Northwestern Univ., Illinois.

Barton, N., Lien, R. & Lunde, J. 1974. Engineering classification of rockmasses for the design of tunnel support. Rock Mechanics, 6 (4): 189-236.

Barton, N. 1976. The shear strength of rock and rock joints. Int. Jour. Rock Mech. Min. Sci. and Geomech. Abstr., 13 (9): 255-279. Also NGI-Publ. 119, 1978.

Barton, N. & Choubey, V. 1977. The shear strength of rock joints in theory and practice. Rock Mechanics, Springer, Vienna, No.1/2: 1-54. Also NGI-Publ. 119, 1978.

Barton, N. & Kjærnsli, B. 1981. Shear strength of rockfill. J. of the Geotech. Eng. Div., Proc. of ASCE, 107 (GT7) Proc. Paper 16374, July: 873-891.

Barton, N. 1982. Modelling rock joint behaviour from in situ block tests: implications for nuclear waste repository design. Office of Nuclear Waste Isolation, Columbus, OH, 96 p., ONWI-308, Sept. 1982.

Barton, N., Bandis, S. & Bakhtar, K. 1985. Strength, deformation and conductivity coupling of rock joints. Int. J. Rock Mech. & Min. Sci. & Geomech. Abstr. 22 (3): 121-140.

Barton, N. 1986. Deformation phenomena in jointed rock. 8th Laurits Bjerrum Memorial Lecture, Oslo. Geotechnique, 36 (2): 147-167.

Barton, N. & Grimstad, E. 1994. The Q-System following twenty years of application in NMT support selection. 43rd Geomechanic Colloquy, Salzburg. Felsbau, 6/94: 428-436.

Barton, N., By, T.L., Chryssanthakis, P., Tunbridge, L., Kristiansen, J., Løset, F, Bhasin, R.K., Westerdahl, H. & Vik, G. 1994. Predicted and measured performance of the 62m span Norwegian Olympic Ice Hockey Cavern at Gjøvik. Int. J. Rock Mech. Min. Sci. & Geomech. Abstr., 31 (6): 617-641. Pergamon.

Barton, N. 1995. The influence of joint properties in modelling jointed rock masses. Keynote Lecture, 8th ISRM Congress, Tokyo, Vol. 3.

Barton, N. & Quadros, E.F. 1997. Joint aperture and roughness in the prediction of flow and groutability of rock masses. Proc. of NY Rocks '97. Linking Science to Rock Engineering, Ed. K. Kim, Int. J. Rock Mech. and Min. Sci. Vol. 34: No. 3-4: 907-916.

Barton, N.1999a.Rockmass characterization from seismic measurements. Keynote lecture, Proc. SAROCKS '98, 2nd Brazilian Symp. 5th South American Rock Mech. Cong., Santos, Brazil. Eds. L. da Silva et al. Vol. 2.

Barton, N. 1999b. TBM performance estimation in rock using Q_{TBM}. Tunnels and Tunnelling International, London, Sept. 1999.

Barton, N. 2000a. Rock quality and seismic velocity. In Press.

Barton, N. 2000b. TBM tunnelling in jointed and faulted rock. In Press.

Bhasin, R., Barton, N., Grimstad, E., Chryssanthakis, P. & Shende, F.P. 1996. Comparison of predicted and measured performance of a large cavern in the Himalayas. Int. J. Rock Mech. Min. Sci. & Geomech. Abstr., 6: 607-626.

Bieniawski, Z. T. 1989. Engineering rock mass classifications: a complete manual for engineers and geologists in mining, civil and petroleum engineering. J. Wiley.

Chen, C. N. & Guo, G. C. 1997. Rock mass classification and guideline for tunnel convegence. Jour. of Chinese Institute of Civil and Hydraulic Engineering, 9 (3): 359-367.

Chryssanthakis, P., Bhasin, R.K.& Barton, N. 1996. Using NMT principles in predicting performance of a powerhouse in the Himalayas, India. Conf. on Recent Advances in Tunnelling Technology, New Dehli 1996, pp. 143-155.

Coulomb, C. A. 1773. Essai sur une application des règles de maximis et minimis à quelques problèmes de statique relatifs à l'architecture. Mém. Math. Phys. Acad. Roy. Sci., Paris, 5 (7): 343-382 (publ. In 1776)

Cundall, P. A.. Voegele, M. & Fairhurst, C. 1977. Computerized design of rock slopes using interactive graphics for the input and output of geometrical data. Proc. of 16th US Rock Mech. Symp., Univ. Of Minnesota, ASCE, New York: 5-14.

Esaki, T., Ikusada, K. & Aikawa, A. 1995. Surface roughness and hydraulic properties of sheared rock. Proc. of Conf. on Fractured and Jointed Rock Masses Eds. Myer, Cook, Goodman & Tsang, Balkema, Rotterdam: 393-398.

Gale, J. E., Macleod, R., Gutierrez, M. & Makurat, A. 1993. Integration and analyses of coupled stress-flow laboratory test data on natural fractures - MUN and NGI tests. Report to AECL, Monitoba, Canada.

Grimstad, E. & Barton, N. 1993. Updating of the Q-System for NMT. Proc. of Int. Symp. on Sprayed Concrete – Modern Use of Wet Mix Sprayed Concrete for Underground Support, Fagernes, 1993, Eds Kompen, Opsahl and Berg. Norwegian Concrete Association, Oslo.

Gutierrez, M. & Ishihara, K. 1999. Non-coaxiality and energy dissipation in granular materials. Soils and Foundations, Japan (in press).

Gutierrez, M. & Makurat, A. 1997. Coupled HTM modelling of cold water injection in fractured hydrocarbon reservoirs Int. J. Rock Mech. & Min. Sci. 34:3-4, Paper No. 00113.

Hoek, E. & Brown, E.T. 1997. Practical estimates of rock mass strength. Int. J. Rock Mech. & Min. Sci. 34(8): 1165-1186.

Hoek, E., Kaiser, P. K. & Bawden, W. F. 1995. Support of underground excavations in Hard Rock. Balkema, Rotterdam.

Loetscher, T. 1999. Appropriate sanitation in developing countries: the development of a computerized decision aid. Ph. D. Thesis, Univ. Of Queensland, Brisbane, Australia.

Mohr, O. 1882. Über die darstellung des spannungszustandes und des deformationszustandes eines körper-elements. Zivil Ingenieur, 113.

Nelson, P. 1996. Rock engineering for underground civil construction. Rock Mechanics, Eds. Aubertin, Hassani & Mitri, Balkema, Rotterdam.

Nunn, K. R., Barker, R. D. & Bamford, D. 1983. In situ seismic and electrical measurments of fracture anisotropy in the Lincolnshire Chalk. Q. Jl. Engng. Geol. 16: 187-195. Northern Ireland: The Geological Society.

NTH, 1994. Hard rock tunnel boring. Project Report 1-94, NTH/NTNU, Trondheim, Norway.

NGI, 1992. PROFHET – Propagation of Fluids and Heat. NGI Internal Report.

Oda, M., Yamabe, T. & Kamemura, K. 1986. A crack tensor and its relation to wave velocity anisotropy in jointed rock masses. Int. J. Rock Mech. & Min. Sci., 23 (6): 387-397.

Olsson, R. 1998. Mechanical and hydromechanical behaviour of hard rock joints – a laboratory study. Ph. D. Thesis, Chalmers Univ. of Tech., Gøteborg, Sweden.

Olsson, R & Barton, N. 1999. A improved model for hydromechanical coupling during shearing of rock joints. (Submitted for publ.).

Potvin, Y., Hudyma, M. R. & Miller, H. D. S. 1989. Design guidelines for open stope support. Bull. Can. Min. Metall. 82 (926): 53-62.

Quadros, E. F. & Filho, D. C. 1995. Grouting efficiency using directional (3-D) hydraulic tests in Pirapora Dam, Brazil. Proc. 8th Congress of ISRM, Tokyo, Ed. Fujii, Balkema, Rotterdam, 2: 823-826.

Robbins, R.J. 1982. The application of tunnel boring machines to bad rock conditions. Proc. ISRM Symp. Aachen, 2: 827-836, Ed. Wittke, Balkema, Rotterdam

Shen, B. & Barton, N. 1997. The disturbed zone around tunnels in jointed rock masses. Technical Note, Int. J. Rock Mech. & Min. Sci. 34 (1): 117-125.

Wickham, G. E. & Tiedemann, H. R. 1974. Ground support prediction model (R.S.R. concept). Jacob Assoc. TR125, Jan. '74.

Papers referenced from Session 1, 9th ISRM Congress, Paris 1999.

Alfonsi, P., Durville, J.-L. & Rachez, X. 1999. Numerical modelling of a foundation on rock slope using the distinct element method: comparison 2D/3D (In French).

Andersson, H. 1999. Chemical rock grouting – an experimental study on polyurethane foams.

Astolfi, G., Sapigni, M., Barla, G. & Innaurato, N. 1999. Inclines: some rock mechanics and excavation problems in two Italian cases.

Barla, G., Barla, M. & Repetto, L. 1999. Continuum and discontinuum modelling for design analysis of tunnels.

Chikahisa, H., Kobayashi, K., Nakahara, H., Matsumoto, K., Tsutsui, M. & Sakurai, S. 1999. Estimation of measurement results concerning deformation behaviour of large-scale rock cavern used as underground museum in excavation.

Damjanac, B., Fairhurst, C. & Brandshaug, T. 1999. Numerical simulation of the effects of heating on the permeability of a jointed rock mass.

Dasgupta, B., Sharma, M.K.V., Verman, M. & Sharma, V.M. 1999. Design of underground caverns for Tehri hydropower project, India by numerical modelling.

Dershowitz, W., Lee, G., Eiben, T. & Wadleigh, E. 1999. Discrete fracture network approach for thermally assisted gravity segregation enhanced oil recovery.

Escoffier, S., Catel, P. & Giafferi, J.L. 1999. Experience return on the empirical methods of support requirement evaluation during underground excavation projects (In French).

Eriksson, M., Janson, T. & Stille, H. 1999. Validation of grout take models with laboratory experiments and numerical calculations.

Glastonbury, J., Mostyn, G. & Fell, R. 1999. Analysis and prediction of the pre-collapse deformation of cut rock slopes.

Goel, S.C. & Wezenberg, U. 1999. Stability of open stopes at Ashanti Goldfields – Obuasi operations.

Hakala, M., Syrjänen, P., Roinisto, J., Salmelainen, J. & Aartolahti, J.-V. 1999. Rock mechanical design of the Kluuvi underground car park/civil defense shelter.

Hibino, S. & Motojima, M. 1999. Anisotropic behaviour of jointed rock mass around large-scale caverns.

Jang, M., Yang, H.-S. & Chung, S.-K. 1999. Stability analysis of high speed railway tunnel passing through the abandoned mine area.

Li, X., Cui, L. & Roegiers, J.-C. 1999. Temperature induced pore pressure and stresses and their potential impacts on wellbore stability.

Savich, A.I., Bronshtein, V.I., Rechitski, V.I. & Ilyin, M.M. 1999. Problems of geodynamic safety of rock foundation and host rock mass of major power projects of Russia.

Schubert, W., Moritz, B. & Sellner, P. 1999. Tunnelling methods for squeezing ground.

Sjöberg, J. 1999. Analysis of failure mechanisms in high rock slopes.

Syrjänen, P. & Lovén, P. 1999. Geostatistics and block modelling in rock mechanics.

Zettler, A.H., Poisel, R., Preh, A. & Roth, W.1999. Stability analysis using finite difference method.